*Journal of Dynamics and Differential Equations, Vol. 12, No. 4, 2000*

# Resonant Homoclinic Flip Bifurcations

**Ale Jan Homburg**[1,2] **and Bernd Krauskopf**[3,4]

*Received October 19, 1998; revised March 28, 2000*

This paper studies three-parameter unfoldings of resonant orbit flip and inclination flip homoclinic orbits. First, all known results on codimension-two unfoldings of homoclinic flip bifurcations are presented. Then we show that the orbit flip and inclination flip both feature the creation and destruction of a cusp horseshoe. Furthermore, we show near which resonant flip bifurcations a homoclinic-doubling cascade occurs. This allows us to glue the respective codimension-two unfoldings of homoclinic flip bifurcations together on a sphere around the central singularity. The so obtained three-parameter unfoldings are still conjectural in part but constitute the simplest, consistent glueings.

**KEY WORDS:** Homoclinic bifurcation; inclination flip; orbit flip; homoclinic-doubling cascade; cusp horseshoe.

## 1. INTRODUCTION

Homoclinic bifurcations have received a lot of attention because they are closely linked to transitions to chaotic dynamics; see, for example, [GAKS93] and further references therein. Many kinds of homoclinic bifurcaftions have been studied, and probably the best known is the Shil'nikov case of a homoclinic orbit to a saddle-focus equilibrium.

In this paper we are interested in a different setting, namely, a vector field in $\mathbf{R}^3$ with a saddle point with real eigenvalues. This saddle point can be taken to be the origin and we consider the case that there is a one-dimensional unstable manifold and a two-dimensional stable manifold.

[1] Institut für Mathematik I, Freie Universität Berlin, Arnimallee 2–6, 14195 Berlin, Germany.
[2] Present address: KdV Institute for Mathematics, University of Amsterdam, Plantage Muidergracht 24, 1018 TV Amsterdam, The Netherlands. E-mail: alejan@science.uva.nl.
[3] Engineering Mathematics, University of Bristol, University Walk, Bristol BS8 1TR, United Kingdom. E-mail: B.Krauskopf@bristol.ac.uk.
[4] To whom correspondence should be addressed.



1040-7294/00/1000-0807$18.00/0 

A homoclinic orbit occurs if a branch of the unstable manifold lies in the stable manifold. Under certain genericity conditions the homoclinic orbit is of codimension-one where one parameter is needed to obtain an unfolding; see the next section for the technical details. There are two cases of different geometry: when the stable manifold is followed along the homoclinic orbit, it generically forms either a cylinder or a Möbius strip. In the unfolding of this homoclinic bifurcation a periodic orbit is created, but there is no complicated dynamics.

When a second parameter is varied, it is possible to change the orientation of the stable manifold from a cylinder to a Möbius strip, or vice versa. This codimension-two bifurcation is called a *homoclinic flip bifurcation*. It can be brought about in two ways, called an *orbit flip* and an *inclination flip* bifurcation as explained in detail in Section 3. Recently, much progress has been made in finding the codimension-two unfoldings of the homoclinic flip bifurcations; see [KKO93a, KKO93b, HKK94, KKO96, Nau96a, Nau96b, Nii96, San93]. There are essentially three possibilities: no extra bifurcations occur, there appears a curve of two-homoclinic orbits that pass very close to the equilibrium once before closing, and a very complicated bifurcation structure that includes $n$-homoclinic orbits of any period $n$, as well as shift-dynamics through the creation and destruction of a cusp horseshoe (Section 3). Which case occurs depends on the eigenvalues at the saddle point, which need to satisfy certain genericity or nonresonance conditions. We provide a complete overview of the results in the literature in a common notation. In the Appendix we also prove the existence of strong stable foliations and exponential expansions that allow us to reduce the analysis of the codimension-two unfoldings to the study of suitable one-dimensional maps.

After this preparatory work, we come to the main question of what happens when one of the eigenvalue conditions separating the different codimension-two cases is not satisfied. We call this a *resonant homoclinic flip bifurcation*. Apart from being the next logical step in studying homoclinic bifurcations, our motivation was the proof of existence of a cascade of homoclinic-doubling bifurcations in [HKN97], where a homoclinic orbit undergoes successive homoclinic-doublings; see also [OKC00]. Such a cascade was found near a particular resonant homoclinic flip orbit [HKN97]. The following questions arise: What does the codimension-three unfolding of such resonant homoclinic flip bifurcations look like? What role does the homoclinic-doubling cascade play in it?

In Section 4 we establish near which cases of a resonant homoclinic flip bifurcation a homoclinic-doubling cascade occurs. What role it plays in the unfoldings of resonant homoclinic flip bifurcations is shown in Section 5, where we present in Figs. 9 through 15 three-parameter unfoldings

of all possible cases. To this end, we adopt the topological point of view that has been very useful in the analysis of codimension-three unfoldings of degenerate equilibria of vector fields; examples are [DRS91, KR96]. The idea is to "glue" corresponding codimension-two unfoldings to each other. Imagine a sphere around the origin in parameter space, where the third parameter unfolds the resonance condition. (For convenience it is assumed that the resonant homoclinic flip bifurcation occurs when all three unfolding parameters are zero.) At the "north pole" of the sphere one finds a particular (and known) unfolding of a codimension-two homoclinic flip bifurcation, and since the eigenvalues of the saddle point are different in the "southern hemisphere," at the "south pole" one finds a different unfolding of such a homoclinic flip bifurcation. The task is now to glue these two codimension-two unfoldings to each other on the surface of the sphere. In other words, the question is to find the additional bifurcations, away from the poles that are necessary to get a consistent bifurcation diagram. Under the assumption that the bifurcation set, or at least the parts of it that we are interested in, has cone structure, the bifurcations on the sphere represent the codimension-three unfolding. Although still conjectural, the bifurcation diagrams presented here constitute the simplest, consistent glueings that take into account all known information. Furthermore, we prove that these unfoldings must contain certain ingredients, for example, homoclinic-doubling cascades.

Codimension-two flip bifurcations have been found in several applications, for example, in [Ko95, ZN98], and they can be detected and followed in parameter space with the package AUTO/HomCont [DCFKSW97]. There is also the model system due to Sandstede [San97] in which resonant flip bifurcations can be studied. By monitoring the eigenvalues, resonant flip bifurcations can be detected in applications. We remark that it is much harder to find the unfolding, that is, the complicated structure of other bifurcations near the central singularity. In recent careful numerical studies of Sandstede's model in [OKC00, OKC00b], the results in Section 5 have been confirmed. In particular, the homoclinic-doubling cascade was found and computed for the first time in a smooth vector field in [OKC00]. The studies in [OKC00] also brought out interesting quantitative features and scaling laws, confirming the outcome of an analysis of scaling laws for model families of interval maps in [HY99].

## 2. NOTATION AND BACKGROUND

We now introduce some notation and recall the case of a generic codimension-one homoclinic orbit. Consider a smooth family of vector fields $\{X_\mu\}$ on $\mathbf{R}^3$, where $\mu = (\mu_1, \mu_2, \mu_3) \in \mathbf{R}^3$. By changing coordinates if

necessary, we arrange that the origin of the phase space is a saddle point, independently of $\mu$. We restrict our attention to the situation that $DX_\mu(\mathbf{0})$ has three distinct real eigenvalues, and without loss of generality we assume that the stable manifold $W^{ss,s}(\mathbf{0})$ is two dimensional. Let $\lambda_{ss}$, $\lambda_s$, and $\lambda_u$ be the eigenvalues of $DX_\mu(\mathbf{0})$, which we define by $\lambda_{ss} < \lambda_s < 0 < \lambda_u$. (For notational convenience we often do not indicate dependence on $\mu$.) For later reference, we define the ratios $\alpha = -\lambda_{ss}/\lambda_u$ and $\beta = -\lambda_s/\lambda_u$ of the eigenvalues, which will turn out to be important parameters. (In fact one can scale $\{X_\mu\}$ to achieve that $\lambda_u = 1$ independently of $\mu$.)

Suppose $\mu$ is a homoclinic bifurcation value of the family $\{X_\mu\}$, meaning that $X_\mu$ has a homoclinic orbit. Let $\Gamma_\mu$ denote the homoclinic orbit of $X_\mu$. Then $\Gamma_\mu$ is of codimension-one if

(G1) $\lambda_s + \lambda_u \neq 0$,

(G2) $\Gamma_\mu \not\subset W^{ss}(\mathbf{0})$, and

(G3) $W^{s,u}(\mathbf{0})$ intersects $W^{ss,s}(\mathbf{0})$ transversally along $\Gamma_\mu$.

Here $W^{ss}(\mathbf{0})$ denotes the one-dimensional strong-stable manifold of $\mathbf{0}$ and $W^{s,u}(\mathbf{0})$ is a two-dimensional center-unstable manifold of $\mathbf{0}$; see also [Hom96]. [The local versions of invariant manifolds are denoted "loc" in subscript: $W^{ss,s}_{\mathrm{loc}}(\mathbf{0})$, etc.] Condition (G1) is a nonresonance condition, and (G2) means that $\Gamma_\mu$ must be tangent to the weak stable direction. Condition (G3) requires that the stable manifold $W^{ss,s}(\mathbf{0})$, if followed along $\Gamma_\mu$, returns along the strong stable direction $W^{ss}(\mathbf{0})$. Consequently, there are two possible cases: the resulting surface may be a (topological) cylinder or a Möbius strip, that is, it is either orientable or twisted. In the unfolding a periodic orbit is created, whose linearization of the Poincaré map has two positive or two negative eigenvalues, respectively.

In the bifurcation diagrams in this paper we introduce some notation that allows us to indicate not only the bifurcation curves, but also what periodic orbits bifurcate. This is important to see that the bifurcation diagrams are consistent. Bifurcation curves are labeled to indicate the type of bifurcation as follows. $H^n_x$ stands for a codimension-one $n$-homoclinic orbit (passing $n-1$ times near the origin before closing), where the subscript indicates whether the homoclinic orbit is orientable ($x = o$) or twisted ($x = t$). Furthermore, $PD^n$ denotes a period-doubling bifurcation and $SN^n$ a saddle-node bifurcation of an $n$-periodic orbit. We indicate stability of periodic orbits in the figures through the coding $n^s$ for a stable $n$-orbit (passing $n$ times near the origin) and $n^u$ for an unstable $n$-orbit (of saddle-type). The limit cycles of type $n^s$ can be found by integration or in an experiment, but those of type $n^u$ require more advanced techniques to be detected in a given system.

## 3. CODIMENSION-TWO UNFOLDINGS

If (G2) and (G3) are satisfied, but not (G1) then one has a codimension-two resonant homoclinic orbit. There are two unfoldings depending on whether the homoclinic orbit is orientable or twisted; see Section 3.1. If (G1) is still satisfied, but (G2) or (G3) are not, then (under extra genericity conditions) $\Gamma_\mu$ is a codimension-two homoclinic orbit, called a *flip homoclinic orbit*. If only (G2) is not satisfied, then $\Gamma_\mu$ is called an *orbit flip homoclinic orbit*, meaning that the homoclinic orbit is formed by the strong stable manifold $W^{ss}(\mathbf{0})$ (see Fig. 1). If only (G3) is not satisfied, then $\Gamma_\mu$ is called an *inclination flip homoclinic orbit*, and the stable manifold $W^{ss,s}(\mathbf{0})$, if followed along $\Gamma_\mu$, returns along the weak stable direction $W^s(\mathbf{0})$ as illustrated in Fig. 2.

Different cases of codimension-two unfoldings of the homoclinic flip bifurcations have been studied [KKO93a, KKO93b, HKK94, KKO96, Nau96a, Nau96b, Nii96, San93] and a complete picture has emerged. [Recall that the orientation of $W^{ss,s}(\mathbf{0})$ changes in both cases, hence, the name flip bifurcations.] It is an interesting fact that the orbit flip and the inclination flip lead to much the same unfoldings. There are essentially three possibilities: **A** no extra bifurcations, **B** homoclinic-doubling (the appearance of a curve of two-homoclinic orbits that pass very close to the equilibrium once before closing), and **C** a very complicated bifurcation structure that includes $n$-homoclinic orbits of any period $n$ and shift-dynamics. Which case occurs depends on the ratios $\alpha$ and $\beta$; see Section 3.2.

We now specialize and consider a smooth two-parameter family $\{X_\mu\}$, $\mu = (\mu_1, \mu_2) \in \mathbf{R}^2$, of vector fields on $\mathbf{R}^3$ possessing a hyperbolic singularity in the origin $\mathbf{0}$, such that $DX_\mu(\mathbf{0})$ has three distinct real eigenvalues $\lambda_{ss}$, $\lambda_s$,

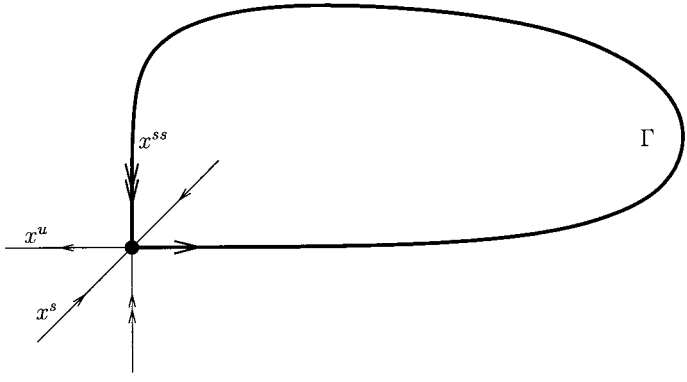


**Fig. 1.** An orbit flip homoclinic orbit.

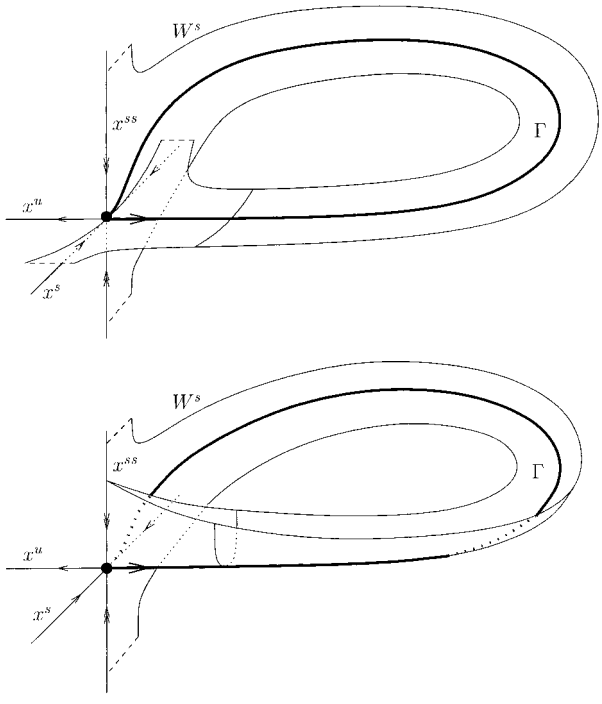


**Fig. 2.** The two cases of an inclination flip homoclinic orbit for $\alpha < 2\beta$ (top) and $\alpha > 2\beta$ (bottom).

and $\lambda_\mu$ with $\lambda_{ss} < \lambda_s < 0 < \lambda_u$. At $\mu = 0$, $X_\mu$ possesses a homoclinic orbit $\Gamma$. Take coordinates $(x_{ss}, x_s, x_u)$ so that

$$DX_\mu(\mathbf{0}) = \lambda_{ss} x_{ss} \frac{\partial}{\partial x_{ss}} + \lambda_s x_s \frac{\partial}{\partial x_s} + \lambda_u x_u \frac{\partial}{\partial x_u} \tag{1}$$

and recall that $\alpha = -\lambda_{ss}/\lambda_u$ and $\beta = -\lambda_s/\lambda_u$.

### 3.1. Homoclinic Orbit at Resonance

Suppose the homoclinic orbit $\Gamma$ of $X_0$ is a homoclinic orbit at resonance, that is, (G1) is not satisfied. This bifurcation was treated in [CDF90]; see also [KKO93a, San93]. Natural parameters to study an unfolding of the homoclinic orbit at resonance are $\mu_1 = \beta - 1$ and $\mu_2$, being the signed distance between stable and unstable manifolds, in a cross section. That is, for some small $\delta$ and in local coordinates in which the local stable manifold is given by $\{x_u = 0\}$, we define $\mu_2$ by $W^u(\mathbf{0}) \cap \{x_s = \delta\} = (*, \delta, \mu_2)$. Observe that the primary homoclinic orbit exists for $\mu_2 = 0$.

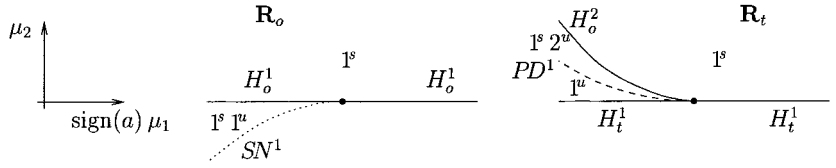


**Fig. 3.** The different cases of unfoldings for the resonant homoclinic bifurcation. Note that $a$ is the constant in the normal form of the return map.

Assuming an additional nondegeneracy condition [CDF90], there are two bifurcation diagrams, depending on whether the homoclinic orbit at $(\mu_1, \mu_2) = (0, 0)$ is orientable or twisted. The bifurcation diagrams are given in Fig. 3.

### 3.2. Flip Homoclinic Orbit

We now summarize the known results on codimension-two homoclinic bifurcations for the cases **A**, **B**, and **C**. For homoclinic flip bifurcations in case **C**, only partial bifurcation diagrams were known. We extend the known results for this case and, in particular, prove the existence of cusp horseshoes and analyze their annihilation.

Suppose $\Gamma$ is a flip homoclinic orbit. Then in the unfolding the primary homoclinic orbit switches from orientable to twisted. Different bifurcation diagrams exist, depending on the values of $\alpha$ and $\beta$ as depicted in Fig. 4. All cases of codimension-two bifurcation diagrams near $\mu = (\mu_1, \mu_2) = (0, 0)$ can be found in Fig. 5.

Case **A** (orbit or inclination flip: $\alpha > \beta > 1$). This case is easily studied using the fact that the Poincaré return map on a cross section is a

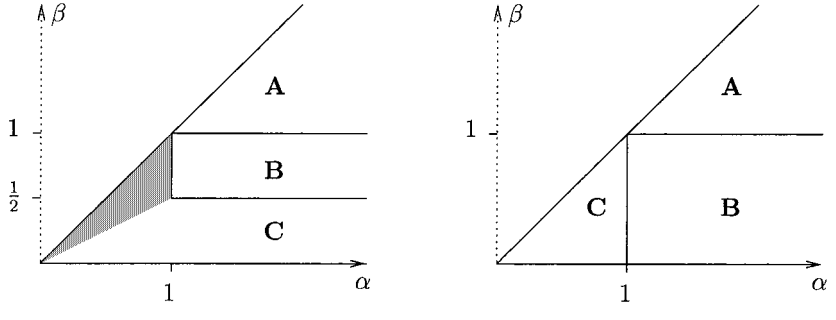


**Fig. 4.** The regions in the $(\alpha, \beta)$-plane of different unfoldings **A**, **B**, and **C** for the orbit flip (right) and the inclination flip (left). The shaded and the unshaded regions of **C** (left) differ by the topology of $W^{ss,s}(\mathbf{0})$ at the inclination flip as shown in Fig. 2.

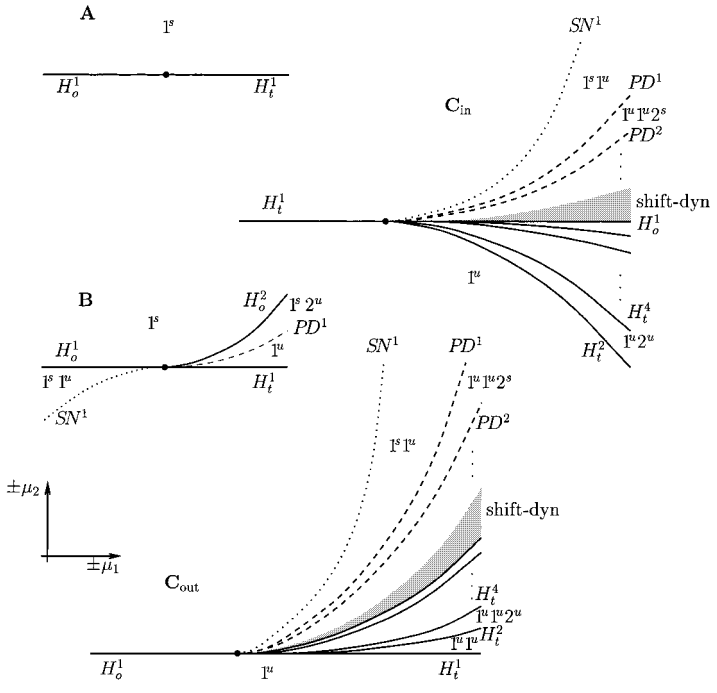


**Fig. 5.** The different cases of unfoldings for the inclination flip and the orbit flip. In **A** no extra bifurcations occur, and **B** is the homoclinic-doubling. The most complicated case, **C**, comes in the two variations $\mathbf{C}_{\text{in}}$ and $\mathbf{C}_{\text{out}}$, depending on how the horseshoe is formed. Stable and unstable periodic orbits of different periods are shown.

contraction. Indeed, it is immediate from this fact that at most one 1-periodic orbit can exist.

Case **B** (orbit flip, $\alpha > 1$, $\beta < 1$; inclination flip, $\alpha > 1$, $1/2 < \beta < 1$). This bifurcation is called a homoclinic-doubling bifurcation. The existence of the depicted bifurcation curves was established for the orbit flip in [San93] and for the inclination flip in [KKO93a, KKO93b, HKN97].

Case **C** (orbit flip, $\beta < \alpha < 1$; inclination flip, $\alpha < 1$ or $\beta < 1/2$). There are two cases, $\mathbf{C}_{\text{in}}$ and $\mathbf{C}_{\text{out}}$. Partial bifurcation diagrams have been obtained in [San93] for the orbit flip and in [Nau96a] for the inclination flip in the region defined by $\alpha < 1$ or $\beta < \frac{1}{2}$. In particular, these references give the existence of curves of $n$-homoclinic orbits, for each integer $n$, in the unfolding. In [HKK94] partial bifurcation diagrams have been obtained in the region $\alpha > 2\beta$ and $\beta < \frac{1}{2}$, under the additional assumption that the vector field near $\mathbf{0}$ is smoothly linearizable. As far as homoclinic bifurcations

are concerned, the bifurcation diagrams in [HKK94] are complete. We remark that Hénon-type strange attractors can be expected to occur in the unfolding; see [Nau96b, Nau98].

We now discuss the orbit flip and the inclination flip separately for $(\alpha, \beta)$ from region **C**. We introduce natural parameters and study the existence and bifurcations of cusp horseshoes. Certain nondegeneracy conditions must be assumed in the bifurcation study, as we will make clear. Our arguments will show that two cases exist, an inward twist case and an outward twist case. This corresponds to the two bifurcation diagrams $\mathbf{C}_{\text{in}}$ and $\mathbf{C}_{\text{out}}$ in Fig. 5. In order to augment the following arguments and provide a complete bifurcation analysis, one needs to address some technical points (like differentiability of strong stable foliations; see Appendix A), which will not be pursued here.

### 3.3. Unfolding of type C of an Orbit Flip

For some small $\delta$, let $\Sigma^{\text{in}}, \Sigma^{\text{out}}$ be the cross sections

$$\Sigma^{\text{in}} = \{x_{ss} = \delta,\ |x_s|,\ |x_u| \leqslant |\delta|\}$$

$$\Sigma^{\text{out}} = \{x_u = \delta,\ |x_{ss}|,\ |x_s| \leqslant |\delta|\}$$

We may assume that they both intersect the homoclinic orbit $\Gamma$ of $X_0$. By a linear rescaling we may assume that $\delta = 1$. Take coordinates $(x_s, x_u)$ on $\Sigma^{\text{in}}$ and $(x_{ss}, x_s)$ on $\Sigma^{\text{out}}$ obtained by restriction of the coordinates $(x_{ss}, x_s, x_u)$ near the origin. Let $\Phi_{\text{loc}}: \Sigma^{\text{in}} \mapsto \Sigma^{\text{out}}$ be the local transition map and let $\Phi_{\text{far}}: \Sigma^{\text{out}} \to \Sigma^{\text{in}}$ be the global transition map. The Poincaré return map $\Phi$ on $\Sigma^{\text{in}}$ is the composition $\Phi = \Phi_{\text{far}} \circ \Phi_{\text{loc}}$. Observe that $\Phi_{\text{far}}$ is a local diffeomorphism. In Appendix B, asymptotic expansions for $\Phi_{\text{loc}}$ are given, valid after a smooth change of coordinates; see Proposition B.5. Using these expansions, we can write

$$\Phi(x_s, x_u) = \begin{pmatrix} \mu_1 + A x_u^{\alpha} + B x_s x_u^{\beta} + \mathcal{O}(x_u^{\alpha+\omega} + x_s^2 x_u^{\beta} + |x_s|\, x_u^{\beta+\omega}) \\ \mu_2 + C x_u^{\alpha} + D x_s x_u^{\beta} + \mathcal{O}(x_u^{\alpha+\omega} + x_s^2 x_u^{\beta} + |x_s|\, x_u^{\beta+\omega}) \end{pmatrix} \tag{2}$$

for some $\omega > 0$. This also identifies the two parameters $\mu_1$ and $\mu_2$: $(\mu_1, \mu_2) = \Phi(0, 0)$ are the coordinates of the first intersection of $W^u(\mathbf{0})$ with $\Sigma^{\text{in}}$.

We assume that $C \neq 0$; the case $C = 0$ corresponds to an inclination flip. We also assume $D \neq 0$. The degenerate case $D = 0$ is called a weak orbit flip [Nau96a]. Let us give an equivalent formulation of this last

nondegeneracy condition. At the bifurcation point $(\mu_1, \mu_2) = (0, 0)$, the image $\Phi_{\text{far}}^{-1}(W_{\text{loc}}^{ss,s}(\mathbf{0}) \cap \Sigma^{\text{in}}) \subset W^{ss,s}(\mathbf{0}) \cap \Sigma^{\text{out}}$ is the graph of a map

$$t \mapsto (at + \mathcal{O}(t^2), t)$$

Then $a \neq 0$ precisely if $D \neq 0$.

We now show that $\Phi$ possesses horseshoes for parameter values $(\mu_1, \mu_2)$ from a wedge, indicated in Fig. 5 as a shaded region. The size of these horseshoes shrinks to 0 as $\mu_1 \to 0$. A suitable rescaling brings these horseshoes to unit size, which fascilitates a study of their properties and bifurcations. We will now give the proper rescaling and indicate how this enables a study of the horseshoes. Let rescaled coordinates $(\bar{x}_s, \bar{x}_u)$ be given by

$$x_s = \mu_1 + |\mu_1|^{\nu} \bar{x}_s$$
$$x_u = |\mu_1|^{\sigma} \bar{x}_u$$

where $\sigma = 1/(\alpha - \beta)$ and $\nu = \alpha/(\alpha - \beta)$. A computation yields the following result.

***Proposition 3.1.*** *Let $\bar{\Phi}$ be the Poincaré return map in the rescaled coordinates $(\bar{x}_s, \bar{x}_u)$. Write $s = \mu_2 |\mu_1|^{-\alpha/(\alpha-\beta)}$. Then, for some $\omega > 0$,*

$$\bar{\Phi}(\bar{x}_s, \bar{x}_u) = \begin{pmatrix} A\bar{x}_u^{\alpha} + B\bar{x}_u^{\beta} + \mathcal{O}(|\mu_1|^{\omega} \bar{x}_u^{\beta}) \\ |\mu_1|^{(\alpha-1)/(\alpha-\beta)} (s + C\bar{x}_u^{\alpha} + D \operatorname{sign}(\mu_1) \bar{x}_u^{\beta} + \mathcal{O}(|\mu_1|^{\omega} \bar{x}_u^{\beta})) \end{pmatrix}$$

This proposition shows that the rescaled Poincaré return map $\bar{\Phi}$ is close to a one-dimensional map, if we take $(\mu_1, \mu_2)$ near 0 from a region in which $s = \mu_2 |\mu_1|^{-\alpha/(\alpha-\beta)}$ is bounded. As $\mu_1 \to 0$, taking $(\bar{x}_s, \bar{x}_u)$ from some compact box $[-l, l] \times [0, k]$, $\bar{\Phi}$ converges to the one-dimensional map

$$\bar{x}_u \mapsto \begin{pmatrix} A\bar{x}_u^{\alpha} + B\bar{x}_u^{\beta} \\ |\mu_1|^{(\alpha-1)/(\alpha-\beta)} g(\bar{x}_u) \end{pmatrix} \tag{3}$$

where

$$g(\bar{x}_u) = s + C\bar{x}_u^{\alpha} + D \operatorname{sign}(\mu_1) \bar{x}_u^{\beta}$$

If $\mu_1 D$ and $C$ have opposite sign, then $\bar{x}_u \mapsto |\mu_1|^{(\alpha-1)/(\alpha-\beta)} g(\bar{x}_u)$ is unimodal and has a graph as depicted in Fig. 8. If the one-dimensional map (3) possesses a horseshoe (when an interval is mapped twice over itself), then also $\Phi$ does for $\mu_1$ small enough and of the correct sign. This

follows from the existence of strong stable foliations; see Appendix A. Straightforward computations yield the existence of an interval of values of $s$, such that $\bar{x}_u \mapsto |\mu_1|^{(\alpha-1)/(\alpha-\beta)}\, g(\bar{x}_u)$ maps two disjoint subintervals of $[0, k]$ onto $[0, k]$, with slope larger than 1 (for suitable large enough $k$ and $l$). For such values of $s$ and $\mu_1$ (corresponding to a wedge shaped region in the $(\mu_1, \mu_2)$ parameter plane), the one-dimensional map (3) has a hyperbolic horseshoe.

The reason for the appearance of two cases, an inward twist case and an outward twist case, follows from a geometric observation. A box $\{0 < \bar{x}_u \leqslant k, |\bar{x}_s| \leqslant l\}$ in the rescaled coordinates corresponds to a small box $D_{\mu_1}$ in the original coordinates, adjacent to the local stable manifold in $\Sigma^{\text{in}}$. The image $\Phi_{\text{far}}^{-1}(D_{\mu_1})$ is on one side of the intersection of $W^{ss,s}(\mathbf{0})$ with $\Sigma^{\text{out}}$ (more precisely, of $\Phi_{\text{far}}^{-1}(W^{ss,s}_{\text{loc}}(\mathbf{0}) \cap \Sigma^{\text{in}})$), which yields the two cases. In Fig. 6 one case is indicated, where the horseshoe exists if $\mu_2 = 0$ (note that the horseshoe is depicted in $\Sigma^{\text{out}}$). This case we call the inward twist case $\mathbf{C}_{\text{in}}$. It is clear that $\Phi$, restricted to $D_{\mu_1}$, does not possess a horseshoe if the image $\Phi_{\text{far}}^{-1}(D_{\mu_1})$ lies on the other side of $W^{ss,s}(\mathbf{0}) \cap \Sigma^{\text{out}}$, at $\mu_2 = 0$. However, by varying the value of $\mu_2$, a horseshoe will be created. This case is called the outward twist case $\mathbf{C}_{\text{out}}$. Which case occurs can be read off from the sign of $C$ in (2): $C > 0$ corresponds to the outward twist case, whereas $C < 0$ corresponds to the inward twist case. The inward and outward twist cases lead to different one-dimensional maps: for the inward twist case, the one-dimensional map $g$ is unimodal with a maximum, whereas for the outward twist case it is unimodal with a minimum; see Fig. 8.

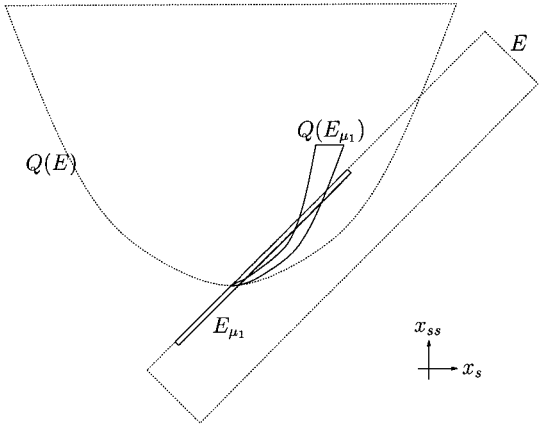


**Fig. 6.** The shape of the cusp horseshoe as it occurs in the unfolding of an orbit flip, lying in the cross section $\Sigma^{\text{out}}$. A small subdomain $E_{\mu_1}$ of the domain $E$ of the return map $Q$ on $\Sigma^{\text{out}}$ is mapped by $Q$ into a horseshoe shape over itself.

Analysis of the rescaled return map $\bar{\Phi}$ enables a characterization of the sequence of homoclinic bifurcations in which the horseshoe annihilates. Varying $s$, one encounters interval maps as in Fig. 8 that do not possess a full horseshoe, since there are no two subintervals that are mapped onto the whole interval. An analysis of such interval maps explains the sequences of bifurcations in which the horseshoe is destructed; see [HKK94, Hom96]. The rescaled return map $\bar{\Phi}$ has the same bifurcation structure as the one-dimensional map (3) as far as the homoclinic bifurcations are concerned. Appendix A contains information on this annihilation process of the horseshoe and the ensuing combinatorics of periodic orbits.

### 3.4. Unfoldings of Type C of an Inclination Flip

For the inclination flip, we follow the same program as for the orbit flip. We will be briefer than in the previous subsection and pay attention mainly to reductions to one-dimensional maps. The rest of the arguments can be filled in by following the reasoning for the orbit flip.

For some small $\delta$, let $\Sigma^{\text{in}}$, $\Sigma^{\text{out}}$ be the cross sections

$$\Sigma^{\text{in}} = \{x_s = \delta,\ |x_{ss}|,\ |x_u| \leqslant |\delta|\}$$
$$\Sigma^{\text{out}} = \{x_u = \delta,\ |x_{ss}|,\ |x_s| \leqslant |\delta|\}$$

intersecting the homoclinic orbit $\Gamma$ of $X_0$. By a linear rescaling we may assume that $\delta = 1$. Take coordinates $(x_{ss}, x_s)$ on $\Sigma^{\text{out}}$ and $(x_{ss}, x_u)$ on $\Sigma^{\text{in}}$ obtained by restriction of the coordinates $(x_{ss}, x_s, x_u)$ near the origin. Let $\Phi_{\text{loc}}: \Sigma^{\text{in}} \mapsto \Sigma^{\text{out}}$ be the local transition map. Let $\Phi_{\text{far}}: \Sigma^{\text{out}} \mapsto \Sigma^{\text{in}}$ be the global transition map, which is a local diffeomorphism. The Poincaré return map $\Phi$ on $\Sigma^{\text{in}}$ is again the composition $\Phi = \Phi_{\text{far}} \circ \Phi_{\text{loc}}$.

The case $\alpha = 2\beta$ is degenerate, and we assume that $\alpha - 2\beta \neq 0$. The two cases with different sign of $\alpha - 2\beta$ are treated separately; see also Fig. 2.

**The Case $\alpha > 2\beta$, $\beta < 1/2$.** Proposition B2 in Appendix B provides asymptotic expansions for the local transition map $\Phi_{\text{loc}}$. Because $\Phi_{\text{far}}$ is a local diffeomorphism, one can write the following expression for $\Phi = \Phi_{\text{far}} \circ \Phi_{\text{loc}}$:

$$\Phi(x_{ss}, x_u) = \begin{pmatrix} p + Bx_u^{\beta} + \mathcal{O}(x_u^{\beta+\omega}) \\ \mu_2 + \mu_1 x_u^{\beta} + Dx_u^{2\beta} + \mathcal{O}(|\mu_1|\, x_u^{\beta+\omega} + x_u^{2\beta+\omega}) \end{pmatrix} \tag{4}$$

for some $\omega > 0$. This also identifies the parameters $(\mu_1, \mu_2)$. For generic families the constant $D$ is nonzero at $(\mu_1, \mu_2) = (0, 0)$, which we assume to be the case.

As above, we will use a rescaling to study the existence of hyperbolic horseshoes. Consider rescaled coordinates $(\bar{x}_{ss}, \bar{x}_u)$ given by

$$x_u = |\mu_1|^\sigma \bar{x}_u$$
$$x_{ss} - p = |\mu_1| \bar{x}_{ss}$$

where $\sigma = 1/\beta$.

***Proposition 3.2.*** *Let $\bar{\Phi}$ be the Poincaré return map in the rescaled coordinates $(\bar{x}_x, \bar{x}_u)$. Write $s = \mu_2 |\mu_1|^{-2}$. Then, for some $\omega > 0$,*

$$\bar{\Phi}(\bar{x}_{ss}, \bar{x}_u) = \begin{pmatrix} B\bar{x}_u^\beta + \mathcal{O}(|\mu_1|^\omega \bar{x}_u^\beta) \\ |\mu_1|^{2-1/\beta} (s + \text{sign}(\mu_1) \bar{x}_u^\beta + D\bar{x}_u^{2\beta} + \mathcal{O}(|\mu_1|^\omega \bar{x}_u^\beta)) \end{pmatrix}$$

As $\mu_1 \to 0$, restricting $\bar{x}_u$ to a compact interval and parameters $(\mu_1, \mu_2)$ to a region in which $s$ is bounded, $\bar{\Phi}$ converges to the one-dimensional map

$$\bar{x}_u \mapsto \begin{pmatrix} B\bar{x}_u^\beta \\ |\mu_1|^{2-1/\beta} (s + \text{sign}(\mu_1) \bar{x}_u^\beta + D\bar{x}_u^{2\beta}) \end{pmatrix}$$

This map is analyzed as before. The return map $\Phi$ has a horseshoe if the one-dimensional map does, by the existence of strong stable foliations; see Appendix A. Figure 7 (top) gives an idea of the geometry of the horseshoe. Note that the horseshoe is drawn in $\Sigma^{\text{out}}$. The inward case is depicted, where the horseshoe exists if $\mu_2 = 0$.

**The Case $\alpha < 2\beta$, $\alpha < 1$.** Applying Proposition B2 from Appendix B, we can write

$$\Phi(x_{ss}, x_u) = \begin{pmatrix} p + Ax_{ss} x_u^\alpha + Bx_u^\beta + \mathcal{O}(x_u^{\alpha+\omega}) \\ \mu_2 + Cx_{ss} x_u^\alpha + \mu_1 x_u^\beta + \mathcal{O}(x_u^{\alpha+\omega}) \end{pmatrix} \tag{5}$$

for some $\omega > 0$. We assume $p \neq 0$; the case $p = 0$ is called a weak inclination flip [Nau96a].

Consider rescaled coordinates $(\bar{x}_{ss}, \bar{x}_u)$ given by

$$x_u = |\mu_1|^\sigma \bar{x}_u$$
$$x_{ss} - p = |\mu_1| \bar{x}_{ss}$$

where $\sigma = 1/(\alpha - \beta)$.

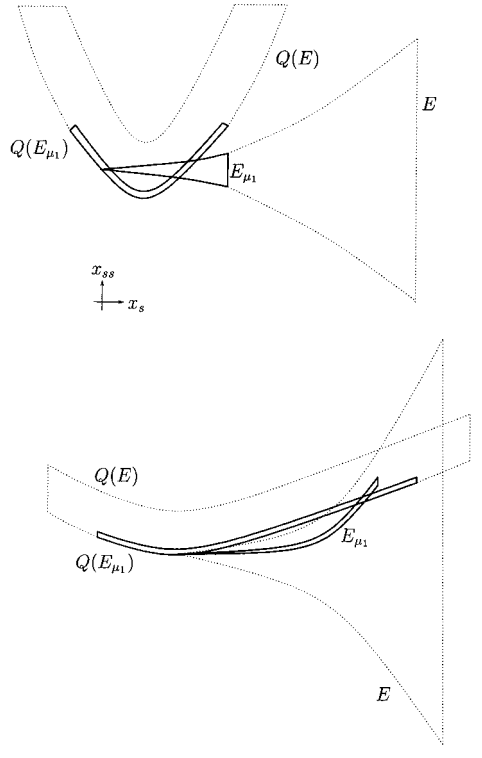


**Fig. 7.** Cusp horseshoe in the unfolding of the inclination flip. The top picture is for $\alpha > 2\beta$ and $0 < \beta < \frac{1}{2}$ and shows the inward twist $\mathbf{C}_{\text{in}}$. The bottom picture is for $\alpha < 2\beta$ and $\alpha < 1$ and shows the outward twist $\mathbf{C}_{\text{out}}$. In both cases a small subdomain $E_{\mu_1}$ of the domain $E$ of the return map $Q$ on $\Sigma^{\text{out}}$ is mapped by $Q$ into a horseshoe shape over itself.

***Proposition 3.3.*** *Let $\bar{\Phi}$ be the Poincaré return map in the rescaled coordinates $(\bar{x}_s, \bar{x}_u)$. Write $s = \mu_2 \, |\mu_1|^{-\alpha/(\alpha-\beta)}$. Then, for some $\omega > 0$,*

$$\bar{\Phi}(\bar{x}_{ss}, \bar{x}_u) = \begin{pmatrix} \mathcal{O}(|\mu_1|^{\omega} \bar{x}_u^{\beta}) \\ |\mu_1|^{(\alpha-1)/(\alpha-\beta)} (s + C(p + |\mu_1| \, \bar{x}_{ss}) \bar{x}_u^{\alpha} + \text{sign}(\mu_1) \bar{x}_u^{\beta} + \mathcal{O}(|\mu_1|^{\omega} \bar{x}_u^{\beta})) \end{pmatrix}$$

As $\mu_1 \to 0$, the map $\bar{\Phi}$ converges to the one-dimensional map

$$\bar{x}_u \mapsto \begin{pmatrix} 0 \\ |\mu_1|^{(\alpha-1)/\alpha-\beta)} \, (s + Cp\bar{x}_u^{\alpha} + \text{sign}(\mu_1) \, \bar{x}_u^{\beta}) \end{pmatrix}$$

A similar analysis as before yields the existence of hyperbolic horseshoes. Figure 7 (bottom) gives an idea of the geometry of the horseshoe. Note

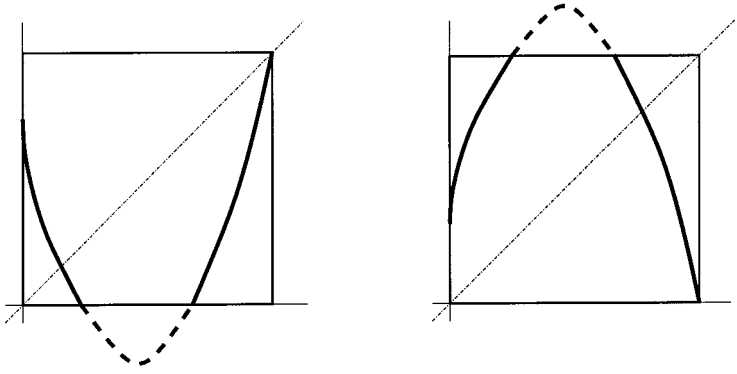

**Fig. 8.** The one-dimensional maps occurring in reductions of homoclinic flip bifurcations for $(\alpha, \beta)$ from region **C** are unimodal. They possess either a minimum for the outward twist case $\mathbf{C}_{\text{out}}$ (left) or a maximum for the inward twist case $\mathbf{C}_{\text{in}}$ (right). Note the infinite derivative at the left end of the graphs.

that the horseshoe is drawn in $\Sigma^{\text{out}}$. The outward case is depicted, where the horseshoe does not exist if $\mu_2 = 0$.

## 4. THE HOMOCLINIC-DOUBLING CASCADE

As mentioned in the Introduction, one of the motivations for writing this paper was the result in [HKN97] that near a particular orbit flip homoclinic orbit of codimension-three, cascades of homoclinic-doubling bifurcations occur. Here, a homoclinic-doubling bifurcation is a codimension-two homoclinic bifurcation with a bifurcation diagram as in case **B** in Fig. 5. Pathfollow a curve of homoclinic bifurcations in the parameter plane. At a homoclinic-doubling bifurcation, continue pathfollowing the curve of doubled homoclinic orbits. A cascade of homoclinic-doubling bifurcations is present if one encounters homoclinic-doubling bifurcations $\mu_n$ in which a $2^n$ homoclinic orbit is created, for all positive integers $n$.

In [HKN97] it was established that such homoclinic-doubling cascades can occur persistently in two-parameter families of vector fields. In fact, an open set of two-parameter families of vector fields that contain cascades of homoclinic-doubling bifurcations is constructed. The members of the families from this open set are near a vector field with a particular resonant orbit flip homoclinic orbit.

***Theorem 4.1 ([HKN97]).*** *Let* $\{X_\mu\}$, $\mu = (\mu_1, \mu_2, \mu_3)$, *be a three-parameter family of vector fields unfolding an orbit flip at resonance* $\alpha = 1$ *with* $\frac{1}{2} < \beta < 1$. *Suppose the number C in (2) is large enough. Let* $\mu_1, \mu_2$ *be*

*defined as in Section 3.3 and let* $\mu_3 = \alpha - 1$. *For each* $\mu_2$ *sufficiently small and positive, the two-parameter family* $\{Y_{\mu_1,\mu_3}\}$, *given by* $Y_{\mu_1,\mu_3} = X_{\mu_1,\mu_2,\mu_3}$, *possesses a connected set of homoclinic bifurcation values in the* $(\mu_1, \mu_3)$*-parameter plane, containing a cascade* $(\mu_1^n, \mu_3^n)$ *of homoclinic-doubling bifurcations in which a* $2^n$*-homoclinic orbit is created. All these homoclinic-doubling bifurcations are inclination flips of type* **B**.

It is not known whether the homoclinic bifurcations in these families are unfolding generically, so that the set of homoclinic bifurcation values might be more complicated than a union of curves. For families from a residual subset of the constructed open set, homoclinic bifurcations will unfold generically. Of basic importance in the derivation of Theorem 4.1 is the observation that a Poincaré return map on a cross section transverse to the homoclinic orbit is close to a one-dimensional map for a subset of the parameters $(\mu_1, \mu_2, \mu_3)$. Recall from Section 3.3 the following expression for the rescaled return map $\bar{\Phi}$:

$$\bar{\Phi}(\bar{x}_s, \bar{x}_u) = \begin{pmatrix} A\bar{x}_u^{\alpha} + B\bar{x}_u^{\beta} + \mathcal{O}(|\mu_1|^{\omega}\, \bar{x}_u^{\beta}) \\ |\mu_1|^{\mu_3/(\alpha-\beta)}\,(s + C\bar{x}_u^{\alpha} + D\,\mathrm{sign}(\mu_1)\,\bar{x}_u^{\beta} + \mathcal{O}(|\mu_1|^{\omega}\,\bar{x}_u^{\beta})) \end{pmatrix}$$

for some $\omega > 0$. Here $s = \mu_2\,|\mu_1|^{-\alpha/(\alpha-\beta)}$. Write $\lambda = |\mu_1|^{\mu_3/(\alpha-\beta)}$ and note that $\lambda = 1$ if $\mu_3 = 0$. Restrict parameter values to a region in which $s$ is bounded and $\lambda$ is bounded and bounded away from 0. Then $\bar{\Phi}$ is a perturbation from the one-dimensional map

$$\bar{x}_u \mapsto \begin{pmatrix} A\bar{x}_u + B\bar{x}_u^{\beta} \\ \lambda(s + C\bar{x}_u + D\,\mathrm{sign}(\mu_1)\,\bar{x}_u^{\beta}) \end{pmatrix}$$

of which only the second coordinate is of importance. Observe that this reduction actually yields a family of maps, depending on the two parameters $\lambda$ and $s$. The rescaled return map $\bar{\Phi}$ has $\mu_1$ as a third and small parameter.

By the eigenvalue condition $\frac{1}{2} < \beta < 1$, an inclination flip occuring for $\mu_3 > 0$ is a homoclinic-doubling bifurcation with a bifurcation diagram as in case **B** in Fig. 5, whereas an inclination flip occuring for $\mu_3 < 0$ has the complicated bifurcation diagram depicted in case **C** in Fig. 5. This remark is the background for the requirement in Theorem 4.1 that $C$ should be sufficiently large: for $C$ large enough all inclination flips occur for $\mu_3 > 0$, that is, for $\lambda < 1$.

The proof of Theorem 4.1 relies on a study of the above one-dimensional map, combined with a continuation theory for homoclinic orbits as developed in [HKN97]. This continuation theory is reminiscent of a

similar theory developed to follow periodic orbits in [YA83], where a continuation theory for periodic orbits was used to find cascades of period-doublings.

The above reasonings can also be applied to the two kinds of resonant inclination flips. Consider the inclination flip at the resonance $\beta = \frac{1}{2}$ with $\alpha > 1$. Consider the rescaled return map $\bar{\Phi}$ from Proposition 3.2. The term $|\mu_1|^{2-1/\beta}$ in front of the second coordinate of $\bar{\Phi}$ is large for $\beta < \frac{1}{2}$ and equals 1 if $\beta = \frac{1}{2}$. We introduce a third parameter, $\mu_3 = \beta - \frac{1}{2}$, and restrict to parameters for which $\lambda = |\mu_1|^{2-1/(\mu_3+1/2)}$ is bounded and bounded away from zero and $s = \mu_2 |\mu_1|^{-2}$ is bounded. Then $\bar{\Phi}$, for $\mu_1$ small, is a perturbation from the one-dimensional map

$$\bar{x}_u \mapsto \begin{pmatrix} B\sqrt{\bar{x}_u} \\ \lambda(s + \operatorname{sign}(\mu_1)\sqrt{\bar{x}_u} + D\bar{x}_u) \end{pmatrix} \tag{7}$$

which depends on the two parameters $\lambda$ and $s$.

Applying arguments developed in [HKN97] allows us to show the existence of homoclinic-doubling cascades in the unfolding of this resonant inclination flip. Indeed, as mentioned above, the proof of Theorem 4.1 relies on a study of the one-dimensional map obtained from rescaling a Poincaré return map, plus an application of a continuation theory for homoclinic orbits. Since the one-dimensional map for the resonant inclination flip is similar to the one obtained for the resonant orbit flip, the reasoning in [HKN97] goes through, and we obtain the following result.

***Theorem 4.2.*** *Let $\{X_\mu\}$, $\mu = (\mu_1, \mu_2, \mu_3)$, be a three-parameter family of vector fields unfolding an inclination flip at resonance $\beta = \frac{1}{2}$ with $\alpha > 1$. Let $\mu_1, \mu_2$ be defined as in Section 3.4 and let $\mu_3 = \beta - \frac{1}{2}$. Suppose the number $D$ in (4) is large enough. For each $\mu_2$ sufficiently small and positive, the two-parameter family $\{Y_{\mu_1,\mu_3}\}$, given by $Y_{\mu_1,\mu_3} = X_{\mu_1,\mu_2,\mu_3}$, possesses a connected set of homoclinic bifurcation values in the $(\mu_1, \mu_3)$-parameter plane, containing a cascade $(\mu_1^n, \mu_3^n)$ of homoclinic-doubling bifurcations in which a $2^n$-homoclinic orbit is created. All these homoclinic-doubling bifurcations are inclination flips of type* **B**.

In one respect the homoclinic-doubling cascades in the unfolding of this resonant inclination flip differ from those occuring in the unfolding of the resonant orbit flip. Namely, in the limit $\mu_1 = 0$ the rescaled return map becomes the one-dimensional map (7) which does not possess homoclinic-doubling cascades. We expect homoclinic-doubling bifurcations in a cascade to occur very close to each other if $\mu_1$ is small; compare the discussion in [HKN97] and in Section 5.4.

The inclination flip at the resonance $\alpha = 1$ with $\frac{1}{2} < \beta < 1$ can be treated in the same way. The rescaled return map $\bar{\Phi}$, for $\mu_1$ small, is a perturbation from the one-dimensional map

$$\bar{x}_u \mapsto \begin{pmatrix} 0 \\ \lambda(s + Cp\bar{x}_u + \text{sign}(\mu_1)\, \bar{x}_u^{\beta}) \end{pmatrix} \tag{8}$$

where $\lambda = |\mu_1|^{(\alpha-1)/(\alpha-\beta)}$ and $s = \mu_2\, |\mu_1|^{-\alpha/(\alpha-\beta)}$.

***Theorem 4.3.*** *Let $\{X_\mu\}$, $\mu = (\mu_1, \mu_2, \mu_3)$, be a three-parameter family of vector fields unfolding an inclination flip at resonance $\alpha = 1$ with $\frac{1}{2} < \beta < 1$. Suppose the number Cp in (5) is large enough. Let $\mu_1, \mu_2$ be defined as in Section 3.4 and let $\mu_3 = \alpha - 1$. For each $\mu_2$ sufficiently small and positive, the two-parameter family $\{Y_{\mu_1,\mu_3}\}$, given by $Y_{\mu_1,\mu_3} = X_{\mu_1,\mu_2,\mu_3}$, possesses a connected set of homoclinic bifurcation values in the $(\mu_1, \mu_3)$-parameter plane, containing a cascade $(\mu_1^n, \mu_3^n)$ of homoclinic-doubling bifurcations in which a $2^n$-homoclinic orbit is created. All these homoclinic-doubling bifurcations are inclination flips of type* **B**.

The theorems in this section can be summarized by saying that a homoclinic-doubling cascade can be found near any transition from type **B** to type **C** in Fig. 4 that features inclination flips of type **B** in its vicinity. Due to the lack of inclination flips of type **B**, in the case not covered by the above theorems of a resonant orbit flip for $\alpha = 1$ and $\beta < \frac{1}{2}$ there is no homoclinic-doubling cascade near the transition from **B** to **C**; see also the discussion in the next section.

## 5. CODIMENSION-THREE UNFOLDINGS

In this section we consider the resonant homoclinic flip bifurcations of codimension-three that correspond to $(\alpha, \beta)$ on the lines between the regions **A**, **B**, and **C** in Fig. 4. The central singularity may be an orbit flip or an inclination flip. There are three classes of transitions.

- The transition from **A** to **B**.
- The transition from **B** to **C** involving a homoclinic-doubling cascade. This occurs for $\frac{1}{2} < \beta < 1$ and $\alpha$ near 1 if the central singularity is an orbit flip or an inclination flip. This also occurs for $\beta$ near $\frac{1}{2}$ and $\alpha > 1$ if the central singularity is an inclination flip.
- The transition from **B** to **C** without a homoclinic-doubling cascade, but with an inclination flip of type **C** instead. This occurs for $0 < \beta < \frac{1}{2}$ and $\alpha$ near 1 if the central singularity is an orbit flip.

We take the topological point of view of glueing the respective codimension-two unfoldings from Section 3 to each other on the surface of a sphere. To this end we arrange the parameters in such a way that one codimension-two singularity sits at the north pole, and the other at the south pole. The problem is now to connect the two in a consistent way on the surface of the sphere.

In the figures we project this sphere to the plane as follows. The parameter $\mu_1$ unfolding the twist changes sign along the vertical axis of each bifurcation diagram. Along the circle, corresponding to the bifurcating one-homoclinic orbit $\Gamma$, the parameter $\mu_2$ (breaking $\Gamma$) changes sign. Finally, the parameter $\mu_3$ unfolding the resonance (crossing between the respective regions **A**, **B**, and **C**) changes sign along the horizontal axis. By adjoining the point at infinity the sphere can be retrieved. The labeling of the bifurcation curves and periodic orbits in the figures is explained in Section 2.

Let us indicate in general terms to what extent the bifurcation diagrams are proved or conjectural. When discussing the different cases we add specific information, where we will be most detailed for the bifurcation diagrams showing homoclinic-doubling cascades. We have no proof that bifurcations unfold generically, which would imply that bifurcations of codimension-one appear as smooth curves on the sphere and bifurcations of codimension-two appear as points. Related to this is that we do not show that the bifurcation diagram has cone structure, that is, that bifurcation diagrams on small spheres of differing radius are homotopic. In fact, one cannot expect cone structure in regions with chaotic dynamics. Hence, we assume that bifurcations unfold generically and we ignore isolas. The depicted bifurcation diagrams are consistent, explain the positions of all bifurcation curves branching from the codimension-two homoclinic bifurcations on the poles of the sphere, and are the simplest possible in the sense that removing bifurcation points or curves would make the bifurcation diagram inconsistent. We remark that most of the features are backed up now by numerical studies; see [OKC00, OKC00b].

Drawing the bifurcation diagrams is made possible by the following observations. First, curves of homoclinic bifurcations cannot intersect; $X_\mu$ possesses at most one homoclinic orbit. Since the orbits we consider are confined to a tubular neighborhood of the resonant homoclinic orbit of codimension-three, curves of $n$-homoclinic orbits connect codimension-two homoclinic bifurcation points. A similar remark holds for codimension-one bifurcations of $n$-periodic orbits. Further knowledge on the necessary occurrence of certain bifurcations is derived by looking at the number and stability of periodic orbits and by understanding the fate of individual periodic orbits.

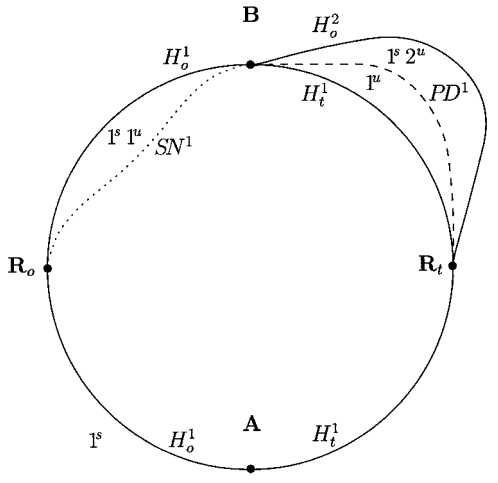


**Fig. 9.** The transition from **A** to **B** involves the orientable and the nonorientable resonant homoclinic bifurcation.

## 5.1. Transition from A to B

We introduce the parameter $\mu_3 = 1 - \beta$, where we fix $\alpha > 1$. The central singularity may be both an orbit flip or an inclination flip. The transition from **A** to **B** when $\mu_3$ changes sign can be resolved on the sphere if one realized that $\mu_1 = \mu_2 = 0$ defines the resonant homoclinic bifurcations from [CDF90] in Fig. 3. There are the two possibilities depending on the sign of a normal form coefficient; see [CDF90]. However, on the sphere both cases are topologically as sketched in Fig. 9. This case was independently studied in [Mon96].

## 5.2. Transition from B to C Involving a Homoclinic-Doubling Cascade

This case was the main motivation for this paper because the homoclinic-doubling cascade was found in [HKN97] near a resonant orbit flip for $\frac{1}{2} < \beta < 1$. In Section 4 we have seen that the homoclinic-doubling cascade is also found near a resonant inclination flip with $\alpha$ near 1 and $\frac{1}{2} < \beta < 1$, and also near a resonant inclination flip with $\beta$ near $\frac{1}{2}$ and $\alpha > 1$. We introduce parameters $(\mu_1, \mu_2, \mu_3)$ as in the respective bifurcation theorems. Recall that the rescalings considered in Section 4 are defined for parameters $(\mu_1, \mu_2, \mu_3)$ from a region for which a function $\lambda$ of the parameters is bounded and bounded away from 0 and a second function $s$

of the parameters is bounded. Recall that for the orbit and inclination flip near the resonance $\alpha = 1$, $\lambda$ and $s$ are given by

$$\lambda = |\mu_1|^{(\alpha-1)/(\alpha-\beta)}$$

$$s = \mu_2 \, |\mu_1|^{-\alpha/(\alpha-\beta)}$$

whereas for the inclination flip near the resonance $\beta = \frac{1}{2}$, $\lambda$ and $s$ are defined by

$$\lambda = |\mu_1|^{2-(1/\beta)}$$

$$s = \mu_2 \, |\mu_1|^{-2}$$

These identities define charts on part of the small sphere around the origin in parameter space. Small neighborhoods of the poles correspond to large and small values of $\lambda$ and are therefore not covered by the charts. But near the poles the bifurcation diagram is that of the codimension-two flip bifurcations, near the north pole of case **C** and near the south pole of case **B**. It remains to study the bifurcations for parameters from the part of the sphere corresponding to large values of $s$. This part of the sphere is not covered by the rescalings from Section 4, but a different rescaling can be used. We discuss this for the resonant orbit flip, but similar considerations apply to the resonant inclination flips.

Let the return map $(x_s, x_u) \mapsto \Phi(x_s, x_u)$ on $\Sigma^{\text{in}}$ be as in (2). Let rescaled coordinates $(\hat{x}_s, \hat{x}_u)$ be given by

$$x_s = \mu_1 + |\mu_2| \, \hat{x}_s$$

$$x_u = |\mu_2|^{1/\alpha} \, \hat{x}_u$$

A computation yields the following result.

***Proposition 5.1.*** *Let $\hat{\Phi}$ be the Poincaré return map in the rescaled coordinates $(\hat{x}_s, \hat{x}_u)$. Write $t = \mu_1 \, |\mu_2|^{(\beta-\alpha)/\alpha}$ and $\nu = |\mu_2|^{(\alpha-1)/\alpha}$. Then, for some $\omega > 0$,*

$$\hat{\Phi}(\hat{x}_s, \hat{x}_u) = \begin{pmatrix} A\hat{x}_u^{\alpha} + Bt\hat{x}_u^{\beta} + \mathcal{O}(|\mu_2|^{\omega} \, \hat{x}_u^{\beta}) \\ \nu(\text{sign}(\mu_2) + C\hat{x}_u^{\alpha} + Dt\hat{x}_u^{\beta} + \mathcal{O}(|\mu_2|^{\omega} \, \hat{x}_u^{\beta})) \end{pmatrix}$$

Take parameter values for which $t$ is bounded (note that small values of $t$ correspond to large values of $s$) and for which $\nu$ is bounded and bounded away from zero (small or large values of $\nu$ occur near the poles on the sphere).

Then for $(\hat{x}_s, \hat{x}_u)$ from a box of the form $[-l, l] \times (0, k]$, the rescaled return map $\hat{\Phi}$ is a perturbation from the one-dimensional map

$$\hat{x}_u \mapsto \begin{pmatrix} A\hat{x}_u + Bt\hat{x}_u^{\beta} \\ \nu(\mathrm{sign}(\mu_2) + C\hat{x}_u + Dt\hat{x}_u^{\beta}) \end{pmatrix}$$

This result, combined with the earlier discussions in Sections 3 and 4, shows that there is a covering of the sphere by charts on which different rescalings to perturbations from one-dimensional maps exist. This enables a bifurcation study for all parameter values on the sphere. Note, however, that the rescalings are applied to $(x_s, x_u)$ from a small box in $\Sigma^{\mathrm{in}}$, whose size goes to 0 as $\mu \to 0$. Bifurcations of orbits outside this box are not captured by an analysis of the rescaled return map; compare the discussion of the codimension-two inclination flip in the appendix of [HKN97].

From a knowledge of the bifurcation structures near the poles and a study of bifurcations of the rescaled return maps from Propositions 3.1 and 5.1, one can draw a consistent bifurcation diagram on the sphere. Recall that we assume that the bifurcations unfold generically and that we ignore isolas of homoclinic or other bifurcations.

The transition from **B** to **C** when $\mu_3$ changes sign is sketched in Figs. 10 and 11 for the two cases $\mathbf{C}_{\mathrm{out}}$ and $\mathbf{C}_{\mathrm{in}}$. These figures certainly need some interpretation. Near the codimension-two point of type **B** a period-two homoclinic orbit is born. As we follow this orbit it undergoes a cascade

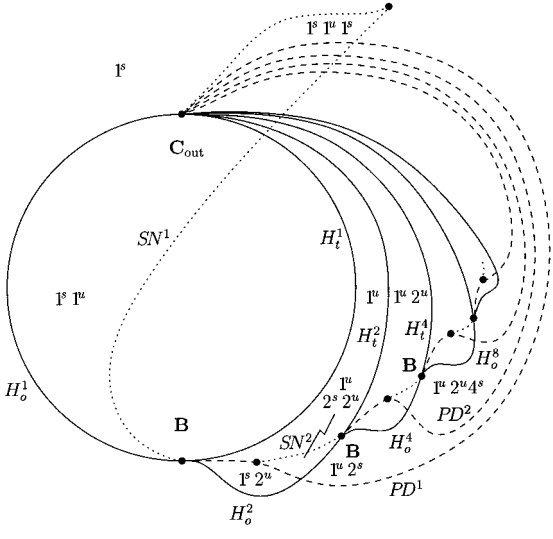


**Fig. 10.** The transition from **B** to $\mathbf{C}_{\mathrm{out}}$ via homoclinic-doubling cascades.

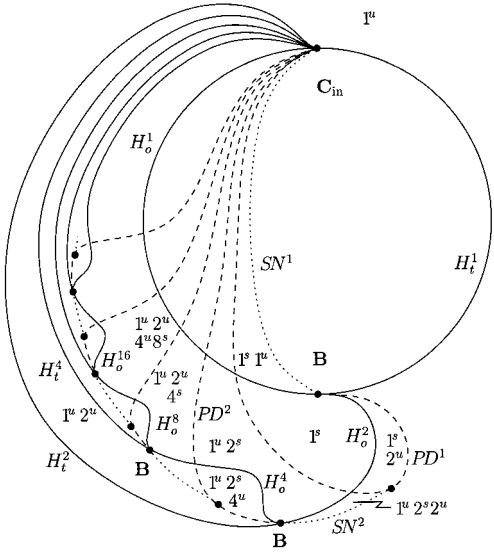


**Fig. 11.** The transition from **B** to $\mathbf{C}_{\text{in}}$ via homoclinic-doubling cascades.

of homoclinic-doublings as described in Section 4. Note that it was shown rigorously that homoclinic-doublings connect to form a complete cascade. The curves of twisted homoclinic loops all end at the codimension-two point of type **C**, as do the curves of period-doublings that are associated with the homoclinic-doubling cascade. By checking the stability of periodic orbits one recognizes that following a curve $PD^{2^k}$ from a homoclinic bifurcation point of type **B** to type $\mathbf{C}_{\text{in}}$ or type $\mathbf{C}_{\text{out}}$, respectively, the period doubling bifurcation has to change from subcritical to supercritical. This implies the existence of a codimension-two point of a degenerate period-doubling of a $2^k$-periodic orbit from which a curve $SN^{2^k}$ branches. Another feature of Fig. 10 is the codimension-two cusp point joining the two branches of the curve $SN^1$ connecting the points **B** and $\mathbf{C}_{\text{out}}$. The importance of the cusp point is explained by noting that **B** and $\mathbf{C}_{\text{out}}$ cannot be end points of a single curve $SN^1$. This in turn is seen by continuing the different 1-periodic orbits that bifurcate from **B** and $\mathbf{C}_{\text{out}}$. We remark that the cusp was found numerically in the study in [OKC00, OKC00b].

The bifurcation curves of homoclinic and periodic orbits described so far account for a part of the bifurcations that occur in the respective unfoldings of the cusp horseshoe in the cases $\mathbf{C}_{\text{out}}$ and $\mathbf{C}_{\text{in}}$. However, they account only for the bifurcations of $2^l$-orbits. We conjecture that there are "$k$-bubbles." configurations of bifurcation curves in which $i$-homoclinic and $i$-periodic orbits are connected, where $i$ is a multiple of $k$. Figures 12 and 13

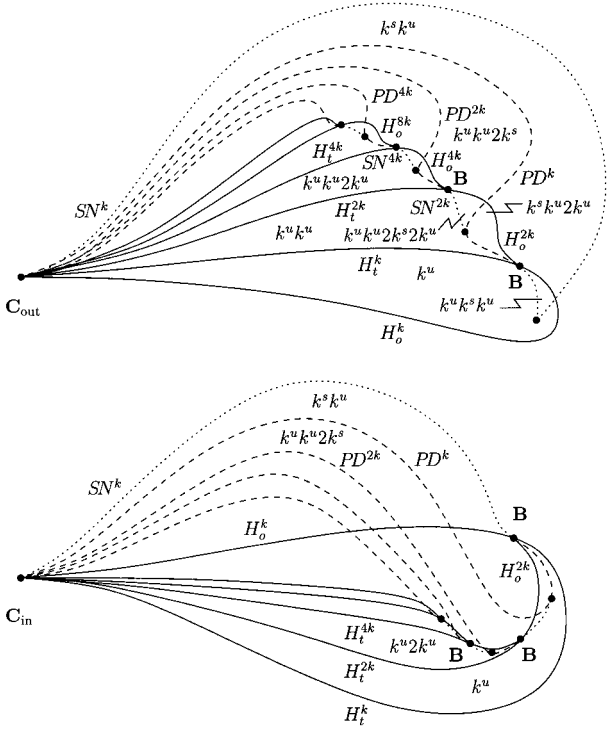


**Fig. 12.** A $k$-bubble with a homoclinic-doubling cascade for the two cases $\mathbf{C}_{\text{out}}$ (top) and $\mathbf{C}_{\text{in}}$ (bottom).

show different $k$-bubbles attached to flip bifurcations of type $\mathbf{C}_{\text{in}}$ and $\mathbf{C}_{\text{out}}$. If the respective coefficient in the expansion of the Poincaré return map occurring in the bifurcation theorems in Section 4 is sufficiently large, we expect to find complete cascades in these $k$-bubbles as in Fig. 12. The $k$-bubbles would then protrude from $\mathbf{C}$ into the lower half-plane where $\mu_3 < 0$: the flip bifurcations in the cascade are inclination flips, which are of type $\mathbf{B}$ only for $\mu_3 < 0$. For smaller values of the coefficient in the expansion of the Poincaré return map, the $k$-bubbles would be situated in $\mu_3 > 0$ and contain two bifurcations of $\mathbf{C}$ type, as indicated in Fig. 13. Combinations with $k$-bubbles consisting of a finite number of homoclinic doubling bifurcations in $\mu_3 < 0$ and an inclination flip of type $\mathbf{C}$ in $\mu_3 > 0$ are another possibility. The existence of $k$-bubbles has been numerically verified in [OKC00b]. The complete bifurcation diagram is now an infinite puzzle of $k$-bubbles that are organized according to the order of bifurcations near $\mathbf{C}_{\text{out}}$ and $\mathbf{C}_{\text{in}}$, respectively. This order is determined by the respective one-dimensional map as explained in Appendix A; see also [HKK94].

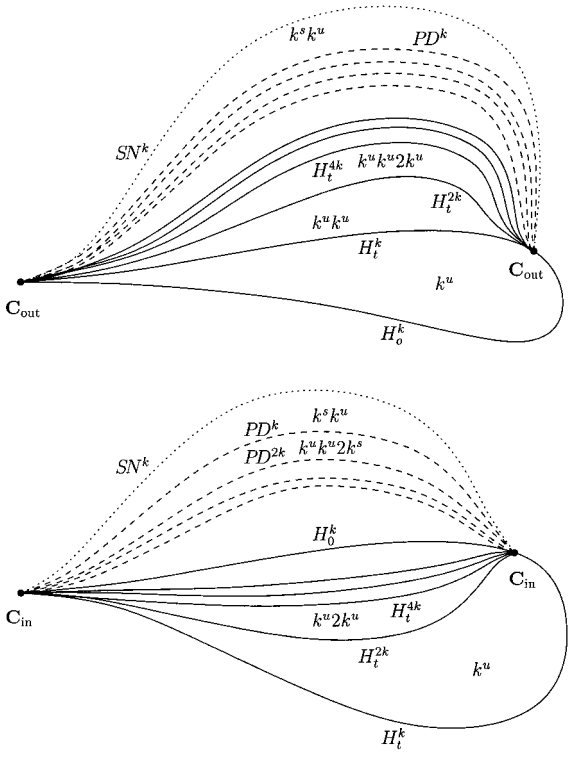


**Fig. 13.** A $k$-bubble without a homoclinic-doubling cascade but with an additional point of type **C** instead. Sketched is the case $\mathbf{C}_{\text{out}}$ with an additional point of type $\mathbf{C}_{\text{out}}$ (top) and the case $\mathbf{C}_{\text{in}}$ with an additional point of type $\mathbf{C}_{\text{in}}$ (bottom).

## 5.3. Transition from B to C Without a Homoclinic-Doubling Cascade

This transition occurs if the central singularity is a resonant orbit flip with $0 < \beta < \frac{1}{2}$. We introduce the parameter $\mu_3 = 1 - \alpha$. Looking at Fig. 4 (right) it is clear that there cannot be a homoclinic-doubling cascade on the sphere, because near the central singularity there are no inclination flips of type **B**. In other words, we must now make the transition from **B** to **C** with inclination flips of type **C**. This means that the point $\beta = \frac{1}{2}$ is a bifurcation point for the codimension-three unfoldings we consider here. We will come back to this point of view below in Section 5.4.

A transition from **B** to $\mathbf{C}_{\text{out}}$ when $\mu_3$ changes sign in this setting is sketched in Fig. 14; a case of a transitions from **B** to $\mathbf{C}_{\text{in}}$ is sketched in Fig. 15. In both figures we consider the situation that the point of type **C** on the curve of 2-homoclinic orbits is of type $\mathbf{C}_{\text{out}}$. The case that this point

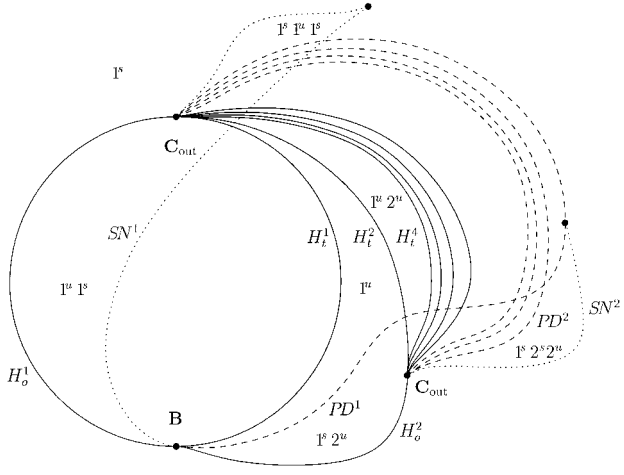


**Fig. 14.** The transition from **B** to $\mathbf{C}_{\text{out}}$ involving an inclination flip of type $\mathbf{C}_{\text{out}}$.

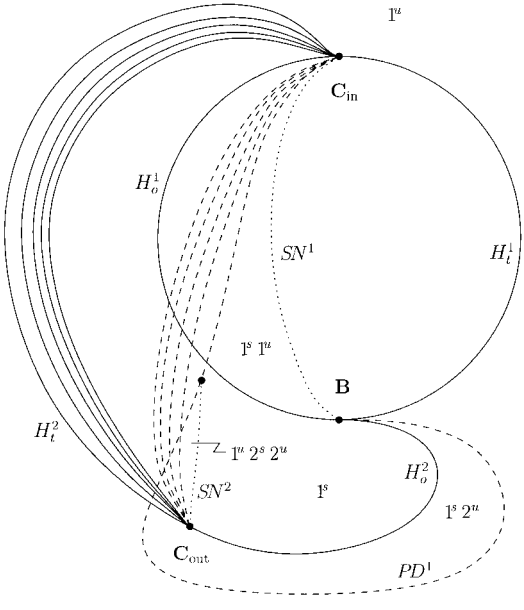


**Fig. 15.** The transition from **B** to $\mathbf{C}_{\text{in}}$ involving an inclination flip of type $\mathbf{C}_{\text{out}}$.

is of type $\mathbf{C}_{\text{in}}$ appears to be possible as well, but this not discussed further here. Transitions from **B** to $\mathbf{C}_{\text{out}}$ via an additional point of $\mathbf{C}_{\text{out}}$ appear in the numerical studies in [OKC00b].

Near the codimension-two point of type **B** a period-two homoclinic orbit is born, but now it undergoes an inclination flip bifurcation of type $\mathbf{C}_{\text{out}}$. The homoclinic loop and period doubling curves all end at the codimension-two point of type $\mathbf{C}_{\text{out}}$. They account for a part of the bifurcations that occur in the respective unfoldings of the cusp horseshoe. We conjecture that there are "$k$-bubbles" as shown in Fig. 13 (top), which also have an inclination flip of type $\mathbf{C}_{\text{out}}$. They account for the bifurcation curves that are missing. The complete bifurcation diagram is again an infinite puzzle of $k$-bubbles that are organized according to the order of bifurcations near the main codimension-two singularity $\mathbf{C}_{\text{out}}$. This order is the same as in the previous case and determined by the one-dimensional map as explained in Appendix A.

### 5.4. From a Homoclinic-Doubling Cascade to a Point of Type $\mathbf{C}_{\text{out}}$

It is of help to consider the transition of the spheres in Figs. 10 and 11 to those in Figs. 14 and 15 as $\beta$ is changed through $\frac{1}{2}$, where the central singularity is an orbit flip. We picture this bifurcation as follows. Let $\frac{1}{2} < \beta$ and consider decreasing $\beta$ toward the bifurcation value $\frac{1}{2}$. Then the successive points in each homoclinic-doubling cascade move closer to each other. (Note that only one parameter should be necessary for this, because it is a reasonable conjecture that there is a scaling law just like in period-doubling.) When $\beta = \frac{1}{2}$ each period doubling cascade has changed to a single point, which is an inclination flip of type **C**. In Figs. 14 and 15 these are inclination flips of type $\mathbf{C}_{\text{out}}$. In order for this to happen, infinitely many cascades of the right combinatorics must all converge to the same point to form this inclination flip of type **C**. We argue now that this ordering is already present "in statu nascendi" for $\frac{1}{2} < \beta$. Because the sphere is compact each homoclinic-doubling cascade has an accumulation point. (We conjecture that there is exactly one such point.) There are clearly infinitely many accumulation points of homoclinic-doubling cascades. We conjecture that the accumulation points of homoclinic-doubling cascades accumulate according to the requirement that they form inclination flips of type **C** as $\beta$ crosses $\frac{1}{2}$. In fact, one could think of the accumulation points of accumulation points of homoclinic-doubling cascades as the seeds for $\frac{1}{2} < \beta$ of the inclination flips of type **C** for $\beta < \frac{1}{2}$. This creation of inclination flips of type **C** might be an explanation for certain computer-generated pictures in [KKO95].

This infinite puzzle requires an infinite number of inclination flips for $\beta > \frac{1}{2}$, which is in accordance with a result in [Nau96a]. Note that these inclination flips of type **C** must also accumulate somewhere on the sphere, making the picture very intricate.

## APPENDIX A: ANNIHILATION OF HORSESHOES

In [HKK94] the destruction of horseshoes through sequences of homoclinic bifurcations in the unfolding of an inclination flip with the eigenvalue conditions $\alpha/\beta > 2$ and $\beta < \frac{1}{2}$ is studied. This is done under a local linearizability assumption. In this appendix we wish to indicate, first, that the results in [HKK94] hold without the local linearizability assumption and, second, that similar bifurcation pictures exist both for the inclination flip with eigenvalue conditions $\alpha/\beta < 2$, $\alpha < 1$, and for the orbit flip with $\beta < \alpha < 1$. For the convenience of the reader we include a characterization of the order of the homoclinic bifurcations in which horseshoes are annihilated, where we follow [HKK94, Hom96].

### A1. Combinatorics of Homoclinic Orbits

Let us start with some considerations on the one-dimensional maps that appear as singular limits after a rescaling; see Section 3. The obtained interval maps (for the different flip homoclinic orbits) are all unimodal with a graph as depicted in Fig. 8. Homoclinic bifurcations of $X_\mu$ correspond to periodic orbits of the interval map that contain 0. This follows from the fact that the local stable manifold of **0** becomes the point 0 in the reduction to the interval map. Note that an $n$-periodic orbit of the interval map that goes through 0 corresponds to an $n$-homoclinic orbit of $X_\mu$. Kneading theory is the tool to obtain information on the set of periodic orbits, and hence, on the set of homoclinic bifurcations, when parameters are varied.

In order to explain this we consider a unimodal map $f_\mu$ as given by (6), (7), or (8) and possessing a minimum as in the left part of Fig. 8. Similar considerations hold for unimodal maps with a maximum. As indicated in the figure, there is an interval $M = [0, m_\mu]$ that is mapped into itself by $f_\mu$; the point $m_\mu$ is the rightmost fixed point of $f_\mu$. Denote by $c_\mu$ the critical point of $f_\mu$. For each point $x$, an itinerary $\mathscr{I}(x)$ is defined as a finite or infinite sequence $\mathscr{I}_j(x)$, $j \geqslant 0$, of symbols $L$ and $R$, according to the following rule:

$$\mathscr{I}_j(x) = \begin{cases} L, & \text{if } f_\mu^j(x) < c_\mu \\ R, & \text{if } f_\mu^j(x) > c_\mu \end{cases}$$

If $f_\mu^j(x)$ is outside of $M$, that is, if $f_\mu^j(x) < 0$ or if $f_\mu^j(x) > m_\mu$, then $\mathscr{I}_k(x)$ is not defined for $k \geqslant j+1$.

One defines an ordering on itineraries as follows. Let $\mathscr{I}, \mathscr{J}$ be two itineraries. Then $\mathscr{I} < \mathscr{J}$ if, for the first integer $j$ with $\mathscr{I}_j \neq \mathscr{J}_j$, the following holds: either $\mathscr{I}_j = L$ and $\mathscr{J} = R$ and the number of $L$'s in $\mathscr{I}_i$, $0 \leqslant i < j$, is odd, or $\mathscr{I}_j = R$ and $\mathscr{J}_j = L$ and the number of $L$'s in $\mathscr{I}_i$, $0 \leqslant i < j$, is even.

Note that $f_\mu^j(x)$ is decreasing at $x$ (and thus changes the order of points close to $x$), precisely if the number of $L$'s in $\mathscr{I}_i(x)$, $0 \leqslant i \leqslant j$, is odd. From this, one deduces that $\mathscr{I}(x) < \mathscr{I}(y)$ implies $x < y$, so that itineraries of points reflect the position on the interval. This observation immediately gives a result on the order of homoclinic bifurcations. First, note that if for $\mu_1$ a fixed small number, one lets $\mu_2$ increase, a horseshoe is created (an interval map is said to have a horseshoe if the interval is mapped twice over itself). Indeed, for $\mu_2 = 0$ we have $f_\mu(0) = 0$ and therefore the invariant set of $f_\mu$ consists of a fixed point in 0 (corresponding to a homoclinic orbit for $X_\mu$) and a fixed point in $m_\mu$ (a periodic orbit for $X_\mu$), whereas for some positive value of $\mu_2$ one has $f_\mu(0) = m_\mu$ and so $f_\mu$ possesses a horseshoe. From the above considerations one concludes that for each $\mathscr{I} < \mathscr{J}$, there are parameter values $\mu_2^1 < \mu_2^2$ (recall that $\mu_1$ is small and fixed), so that 0 is a periodic point both for $f_{(\mu_1, \mu_2^1)}$ and for $f_{(\mu_1, \mu_2^2)}$ and such that $\mathscr{I}(0) = \mathscr{I}$ for $\mu = (\mu_1, \mu_2^1)$ and $\mathscr{I}(0) = \mathscr{J}$ for $\mu = (\mu_1, \mu_2^2)$.

If one further has a monotonicity property of the homoclinic bifurcations, saying that the value of $\mu_2$ (for fixed $\mu_1$) for which 0 is periodic with some prescribed itinerary, is unique, then this fully describes the order of homoclinic bifurcations. That $f_\mu$ has such a monotonicity property follows from

$$\frac{\partial}{\partial \mu_2} f_\mu^n|_x = \sum_{j=0}^{n-1} \frac{d}{dx} f_\mu^j|_{f_\mu^{n-j}(x)} \frac{\partial}{\partial \mu_2} f_\mu|_{f_\mu^{n-j-1}(x)}$$

Indeed, since for $\mu$ small, $|(d/dx)\, f_\mu|_x$ is large, the above expression is non-zero and its sign equals the sign of the dominant term $(d/dx)\, f_\mu^{n-1}|_{f_\mu(x)}$ $(\partial/\partial\mu_2)\, f_\mu|_x$. Applying this to $x = 0$ at a homoclinic bifurcation value shows the required monotonicity.

Following [Hom96], one sees that the first homoclinic bifurcations are of periodic points with itineraries

$$(L)^\infty, \qquad (LR)^\infty, \qquad (LRLL)^\infty, \qquad (LRLLLRLR)^\infty$$

in this order. For each itinerary, the following itinerary is obtained by taking the block of symbols which is periodically repeated, putting two of these blocks behind each other, changing the last symbol of the new obtained

block, and then repeating this block periodically. There are various such sequences of homoclinic bifurcations. Indeed, if $U$ is a block of symbols containing an even number of $L$'s, then there is a sequence of subsequent homoclinic bifurcations with the following itineraries:

$$(UR)^\infty, \qquad (UL)^\infty, \qquad (ULUR)^\infty, \qquad (ULURULUL)^\infty$$

and so on using the same rule as above. A similar sequence of subsequent homoclinic bifurcations exists for blocks of symbols $U$ containing an odd number of $L$'s. Here the order is

$$(UL)^\infty, \qquad (UR)^\infty, \qquad (URUL)^\infty, \qquad (URULURUR)^\infty$$

and so on.

## A2. Strong Stable Foliations

Recall that $f_\mu$ is the singular limit of a rescaled return map $\bar{\Phi}$ as $\mu_1 \to 0$. The above results on the one-dimensional map can be extended to $\bar{\Phi}$ by constructing a strong stable foliation. Identifying points on the same leaf of such a foliation results in a one-dimensional map, close to $f_\mu$ for $\mu$ small. To extend the combinatorial part of the above description to $\bar{\Phi}$, it suffices to construct a continuous strong stable foliation: kneading theory applies to continuous unimodal maps. For statements on monotonicity and genericity of the unfolding of the bifurcations, a continuously differentiable strong stable foliation is required. We do not discuss this issue but refer to [HKK94].

We now prove for the case of the orbit flip that a strong stable foliation for $\bar{\Phi}$ does exist. Similar proofs can be given for the two types of inclination flips. Recall from Section 3 that, for $\mu_1$ small, the rescaled return map $(\bar{x}_s, \bar{x}_u) \mapsto \bar{\Phi}(\bar{x}_s, \bar{x}_u)$ is a singular perturbation from the one-dimensional map

$$\bar{x}_u \mapsto \begin{pmatrix} A\bar{x}_u^\alpha + B\bar{x}_u^\beta \\ |\mu_1|^{(\alpha-1)/(\alpha-\beta)}\, g(\bar{x}_u) \end{pmatrix}$$

where $g(\bar{x}_u) = s + C\bar{x}_u^\alpha + D \operatorname{sign}(\mu_1)\, \bar{x}_u^\beta$.

In order to state the result we consider $(\bar{x}_s, \bar{x}_u)$ on a bounded region $[-l, l] \times (0, k]$, for some $k, l$ large enough. We follow [HKK94]; related or comparable results can further be found in [Rob89, Rob92, Ryc90, Hom96].

***Proposition A1.*** *For some $\lambda > 0$, and $\mu_1 D$ of the opposite sign as $C$, let $W$ be the set of parameter values so that $|g'|_I| \geqslant \lambda$, where $I = \{\bar{x}_u \in (0, k];\ |\mu_1|^{(\alpha-1)/(\alpha-\beta)}\, g(\bar{x}_u) \in (0, k]\}$. For $(\mu_1, \mu_2) \in W$, $\bar{\Phi}$ possesses a continuous strong stable foliation on $[-l, l] \times [0, k]$.*

**Proof.** Instead of studying the Poincaré return map $\Phi$ on $D_{\mu_1} \subset \Sigma^{\text{in}}$ (where $D_{\mu_1}$ is the box that rescales to $[-l, l] \times (0, k]$), we consider the Poincaré return map $\Psi$ on the parameter-dependent cross section

$$S^{\text{in}} = \{x_s = \mu_1,\ |x_{ss}|,\ |x_u| \leqslant 1\}$$

This makes the construction similar to corresponding constructions near inclination flip homoclinic orbits. Note that, for $\mu_2 = 0$, the homoclinic orbit intersects $S^{\text{in}}$ in $(1, \mu, 0)$. For definiteness, we assume that $C$ and $D$ are such that $\mu_1$ is positive. Let

$$E_{\mu_1} = \{0 < x_u \leqslant k\mu_1^{\sigma},\ |x_{ss} - 1| \leqslant l\mu_1^{\nu}\}$$

$\sigma = 1/(\alpha - \beta)$, $\nu = \alpha/(\alpha - \beta)$, be a small box in $S^{\text{in}}$. The existence of a strong stable foliation for $\Phi$ on $D_{\mu_1}$ follows from the existence of a strong stable foliation for $\Psi$ on $E_{\mu_1}$.

A strong stable foliation is obtained by integrating a line field that is invariant under $D\Psi$ and has the property that $D\Psi$ strongly contracts vectors in the direction of the line field. Such a line field is constructed using an appropriate graph transform. We prove the proposition for fixed parameter values. Take rescaled coordinates $(\bar{x}_{ss}, \bar{x}_u) \in [-l, l] \times (0, k]$ on $E_{\mu_1}$ given by

$$x_{ss} - 1 = \mu_1^{\nu} \bar{x}_{ss}$$

$$x_u = \mu_1^{\sigma} \bar{x}_u$$

and let $\bar{\Psi}$ denote the Poincaré return map in these rescaled coordinates. Write $T([-l, l] \times (0, k]) = [-l, l] \times (0, k] \times E^{ss} \times E^u$. Let $\bar{\Psi}^{-1}$ be the map induced by $\bar{\Psi}^{-1}$ on $[-l, l] \times (0, k] \times \mathscr{L}(E^{ss}, E^u)$;

$$\bar{\Psi}^{-1}(\bar{x}_{ss}, \bar{x}_u, \bar{v}) = (\bar{\Psi}^{-1}(\bar{x}_{ss}, \bar{x}_u), \bar{w})$$

with

$$\text{graph } \bar{w} = D\bar{\Psi}^{-1}(\bar{x}_{ss}, \bar{x}_u) \text{ graph } \bar{v}$$

Let $\Gamma$ be the corresponding graph transform on $C^0([-l, l] \times (0, k], \mathscr{L}(E^{ss}, E^u))$, that is, $\Gamma$ is defined by

$$(\bar{x}_{ss}, \bar{x}_u, \Gamma(\bar{v})(\bar{x}_{ss}, \bar{x}_u)) = \bar{\Psi}^{-1}(\bar{\Psi}(\bar{x}_{ss}, \bar{x}_u), \bar{v} \circ \bar{\Psi}(\bar{x}_{ss}, \bar{x}_u))$$

for $(\bar{x}_{ss}, \bar{x}_u)$ such that $\bar{\Psi}(\bar{x}_{ss}, \bar{x}_u) \in [-l, l] \times (0, k]$. For other $(\bar{x}_{ss}, \bar{x}_u)$ we let $\Gamma(\bar{v})(\bar{x}_{ss}, \bar{x}_u) = \bar{v}_0(\bar{x}_{ss}, \bar{x}_u)$ for a fixed section $\bar{v}_0$; see [HKK94, Hom96] for details.

We claim the existence of $\delta > 0$ so that

- $\Gamma$ maps the set $C^0_\delta([-l, l] \times (0, k], \mathscr{L}(E^{ss}, E^u))$ of continuous sections in $C^0([-l, l] \times (0, k], \mathscr{L}(E^{ss}, E^u))$ with supnorm bounded by $\delta$ into itself.
- $\Gamma$ is a contraction on $C^0_\delta([-l, l] \times (0, k], \mathscr{L}(E^{ss}, E^u))$ in the supnorm.

Note that $\bar{\Psi}$ is defined only for $\bar{x}_u > 0$ (and at $\bar{x}_u = 0$ by continuous extension).

In the remainder, we prove the claim. Combining the proofs of Proposition B5 in Appendix B (we are using a different cross section, so that Proposition B5 does not apply directly) and Proposition 3.1, one has

$$\bar{\Psi}(\bar{x}_{ss}, \bar{x}_u) = \begin{pmatrix} A(\bar{x}_{ss})\, \bar{x}_u^{\alpha} + B(\bar{x}_{ss})\, \bar{x}_u^{\beta} + \mathcal{O}(|\mu_1|^{\omega}\, \bar{x}_u^{\beta+\omega}) \\ |\mu_1|^{(\alpha-1)/(\alpha-\beta)} (C(\bar{x}_{ss})\, \bar{x}_u^{\alpha} + D(\bar{x}_{ss}) \operatorname{sign}(\mu_1)\, \bar{x}_u^{\beta} + \mathcal{O}(|\mu_1|^{\omega}\, \bar{x}_u^{\beta+\omega})) \end{pmatrix} \tag{9}$$

for some $\omega > 0$. The higher-order terms can be differentiated, as stated in Proposition B5. The function $A$ is of the form $\tilde{A}(1 + |\mu_1|^{\nu} \bar{x}_{ss})$ for a smooth function $\tilde{A}$, and similarly for $B$, $C$, $D$.

Consider the action of the map $\bar{\Psi}^{-1}$: $\bar{\Psi}([-l, l] \times (0, k]) \times \mathscr{L}(E^{ss}, E^u) \to [-l, l] \times (0, k] \times \mathscr{L}(E^{ss}, E^u)$, induced by $\bar{\Psi}^{-1}$. Write

$$D\bar{\Psi}(\bar{x}_{ss}, \bar{x}_u) = \begin{pmatrix} a(\bar{x}_{ss}, \bar{x}_u) & b(\bar{x}_{ss}, \bar{x}_u) \\ c(\bar{x}_{ss}, \bar{x}_u) & d(\bar{x}_{ss}, \bar{x}_u) \end{pmatrix}$$

Observe that $\bar{\Psi}^{-1}(\bar{\Psi}(\bar{x}_{ss}, \bar{x}_u), w) = (\bar{x}_{ss}, \bar{x}_u, v)$, where $w$ and $v$ are related by

$$\begin{pmatrix} a(\bar{x}_{ss}, \bar{x}_u) & b(\bar{x}_{ss}, \bar{x}_u) \\ c(\bar{x}_{ss}, \bar{x}_u) & d(\bar{x}_{ss}, \bar{x}_u) \end{pmatrix} \begin{pmatrix} 1 \\ v \end{pmatrix} = k \begin{pmatrix} 1 \\ w \end{pmatrix}$$

for some $k \in \mathbf{R}$. This shows that $v$ and $w$ are related by

$$v = \frac{-c(\bar{x}_{ss}, \bar{x}_u) + a(\bar{x}_{ss}, \bar{x}_u)\, w}{d(\bar{x}_{ss}, \bar{x}_u) - b(\bar{x}_{ss}, \bar{x}_u)\, w}$$

So, if $\bar{v} \in C^0(\bar{\Psi}([-l, l] \times (0, k]), \mathscr{L}(E^{ss}, E^u))$, then

$$\Gamma(\bar{v}) = \frac{-c + a\bar{v} \circ \bar{\Psi}}{d - b\bar{v} \circ \bar{\Psi}}$$

Write $\mathscr{O} = \mathscr{O}(|\mu_1|^\omega \bar{x}_u^{\beta+\omega-1})$ and $\mathscr{O}_1 = \mathscr{O}(|\mu_1|^\omega \bar{x}_u^\omega)$. Use (9) to compute

$$\begin{aligned}
\Gamma(\bar{v})(\bar{x}_{ss}, \bar{x}_u) &= \frac{\begin{pmatrix} \mathscr{O} - C'\bar{x}_u^{\alpha-1} - \operatorname{sign}(\mu_1)\, D'\bar{x}_u^{\beta-1} \\ \quad + |\mu_1|^{(1-\alpha)/(\alpha-\beta)} (A'\bar{x}_u^{\alpha-1} + B'\bar{x}_u^{\beta-1} + \mathscr{O})\, \bar{v} \circ \bar{\Psi} \end{pmatrix}}{\begin{pmatrix} \mathscr{O} - C\alpha\bar{x}_u^{\alpha-1} - \operatorname{sign}(\mu_1)\, D\beta\bar{x}_u^{\beta-1} \\ \quad - |\mu_1|^{(1-\alpha)/(\alpha-\beta)} (A\alpha\bar{x}_u^{\alpha-1} + B\beta\bar{x}_u^{\beta-1} + \mathscr{O})\, \bar{v} \circ \bar{\Psi} \end{pmatrix}} \\
&= \frac{\begin{pmatrix} \mathscr{O}_1 - C'\bar{x}_u^{\alpha-\beta} - \operatorname{sign}(\mu_1)\, D' \\ \quad + |\mu_1|^{(1-\alpha)/(\alpha-\beta)} (A'\bar{x}_u^{\alpha-\beta} + B' + \mathscr{O}_1)\, \bar{v} \circ \bar{\Psi} \end{pmatrix}}{\begin{pmatrix} \mathscr{O}_1 - C\alpha\bar{x}_u^{\alpha-\beta} - \operatorname{sign}(\mu_1)\, D\beta \\ \quad - |\mu_1|^{(1-\alpha)/(\alpha-\beta)} (A\alpha\bar{x}_u^{\alpha-1} + B\beta + \mathscr{O}_1)\, \bar{v} \circ \bar{\Psi} \end{pmatrix}}
\end{aligned}$$

Here $A$, $B$, $C$, $D$ and their derivatives are computed in $\bar{x}_{ss}$ and $\bar{v} \circ \bar{\Psi}$ is computed in $(\bar{x}_{ss}, \bar{x}_u)$.

By assumption, $g'(\bar{x}_u) \sim -C\alpha\bar{x}_u^{\alpha-1} - \operatorname{sign}(\mu_1)\, D\beta\bar{x}_u^{\beta-1}$ (the term appearing in the denominator of the above expression) is bounded away from zero. From these facts one derives the claim; see [HKK94]. □

## APPENDIX B: EXPONENTIAL EXPANSIONS

In this appendix we provide exponential expansions for the local transition maps for the vector field $X_\mu$ encountered in Section 3. It is well known that under the assumption of nonresonance conditions on the eigenvalues of $DX_\mu(\mathbf{0})$, there exist smooth coordinates near $\mathbf{0}$ in which $X_\mu$ is linear [Ste58]. For a locally linear vector field an explicit expression for the local transition map can be given. Since we consider resonant flip bifurcations, and thus have rationally dependent eigenvalues, we cannot assume the existence of smooth locally linearizing coordinates. We circumvent this difficulty by computing asymptotic expansions for the local transition maps. This provides a way of studying homoclinic bifurcations without having to rely on the simplifying assumption of smooth local linearizability.

We start with a normal form theorem. Let $X_\mu$ be give by a set of ordinary differential equations,

$$\begin{aligned} \dot{x}_{ss} &= -\alpha x_{ss} + F_{ss}(x_{ss}, x_s, x_u) \\ \dot{x} &= -\beta x_s + F_s(x_{ss}, x_s, x_u) \\ \dot{x}_u &= x_u + F_u(x_{ss}, x_s, x_u) \end{aligned} \tag{10}$$

where $F^{ss}$, $F^s$, $F^u$ are quadratic and higher-order terms.

***Lemma B1.*** *The vector field $X_\mu$ is smoothly equivalent to a vector field of the same form with*

$$\begin{aligned} F_{ss}(x_{ss}, x_s, x_u) &= \mathcal{O}(\|(x_{ss}, x_s)\|^2) \\ F_s(x_{ss}, x_s, x_u) &= x_u \mathcal{O}(|x_{ss}| + \|(x_{ss}, x_s)\|^2) \\ F_u(x_{ss}, x_s, x_u) &= 0 \end{aligned}$$

*Moreover, if $\alpha > 2\beta$, the same is true with*

$$F_{ss}(x_{ss}, x_s, x_u) = \mathcal{O}(x_{ss}^2 + |x_{ss} x_s| + x_s^3) \tag{11}$$

*If $\alpha - \beta < 1$, we can take*

$$F_s(x_{ss}, x_s, x_u) = x_u \mathcal{O}(\|(x_{ss}, x_s)\|^2) \tag{12}$$

**Proof.** By a smooth coordinate change, the local stable and unstable manifolds are linear. Then $F_{ss}$ and $F_s$ are of order $\mathcal{O}(\|(x_{ss}, x_s)\|)$ and $F_u$ is of order $\mathcal{O}(|x_u|)$. Multiplying the vector field with the smooth function $x_u/(x_u + F_u(x_{ss}, x_s, x_u))$, we obtain that $X_\mu$ is smoothly equivalent to a vector field for which $F_u = 0$.

First, by a smooth coordinate transformation, we remove terms $x_{ss}\mathcal{O}(x_u)$ from the differential equation for $x_{ss}$ and terms $x_s\mathcal{O}(x_u)$ from the differential equation for $x_s$. For this, consider a coordinate change $(x_{ss}, x_s, x_u) \mapsto (y_{ss}, y_s, y_u)$ of the form

$$\begin{aligned} y_{ss} &= x_{ss} + p^{ss}(x_u)\, x_{ss} \\ y_s &= x_s + q^s(x_u)\, x_s \\ y_u &= x_u \end{aligned}$$

for functions $p^{ss}$, $p^s$ which vanish at $x_u = 0$. Write the differential equations in the new coordinates $(y_{ss}, y_s, y_u)$ as

$$\begin{aligned}
\dot{y}_{ss} &= -\alpha y_{ss} + G^{ss}(y_{ss}, y_s, y_u)\, y_{ss} + G^s(y_{ss}, y_s, y_u)\, y_s \\
\dot{y}_s &= -\beta y_s + H^{ss}(y_{ss}, y_s, y_u)\, y_{ss} + H^s(y_{ss}, y_s, y_u)\, y_s \\
\dot{y}_u &= y_u
\end{aligned}$$

At $y_{ss}, y_s = 0$, we have

$$\begin{aligned}
G^{ss}(0, 0, y_u) &= \dot{p}^{ss} + h.o.t. \\
H^s(0, 0, y_u) &= \dot{q}^s + h.o.t.
\end{aligned}$$

where *h.o.t.* stands for higher-order terms in $(p^{ss}, q^s, y_u)$; compare [OS87, Den89b]. We seek functions $p^{ss}, q^s$ of $y_u = x_u$ so that $G^{ss}$ and $H^s$ vanish at $y_{ss}, y_s = 0$. Considering $p^{ss}$ and $q_s$ as variables, this yields differential equations for $(p^{ss}, q^s, y_u)$:

$$\begin{aligned}
\dot{p}^{ss} &= h.o.t. \\
\dot{q}^s &= h.o.t. \\
\dot{y}_u &= y_u
\end{aligned}$$

The eigenvalues of the linearized differential equations, at $p^{ss}, q^s, y_u = 0$, are $0, 0, 1$. Hence we obtain the desired functions $p^{ss}, q^s$ by constructing the one-dimensional strong unstable manifold for the above system of differential equations.

On the stable manifold, there exists a strong stable foliation with one-dimensional leaves, extending the strong stable manifold. A smooth coordinate change brings this foliation into an affine foliation. The differential equation for $x_s$ restricted to the stable manifold $\{x_u = 0\}$ depends only on $x_s$. Since one-dimensional vector fields can always be smoothly linearized near a sink, after a smooth coordinate change we get $F_s(x_{ss}, x_s, x_u) = \mathcal{O}(|x_u| \, \|(x_{ss}, x_s)\|)$. Any center unstable manifold $W^{s,u}(\mathbf{0})$ has the same tangent bundle along $W^u(\mathbf{0})$; see for example [Hom96]. By a smooth coordinate change $TW^{s,u}(\mathbf{0})|_{W^u(\mathbf{0})} = T\{x_{ss} = 0\}$. This removes terms $x_s \mathcal{O}(x_u)$ from the differential equation for $x_{ss}$. If $\alpha > 2\beta$, then any $W^{s,u}(\mathbf{0})$ is a $C^2$ manifold and has a unique bundle of 2-jets along $W^u(\mathbf{0})$. A smooth coordinate change makes any $W^{s,u}(\mathbf{0})$ second-order tangent to $\{x_{ss} = 0\}$ along $W^u(\mathbf{0})$. Then also terms $x_s^2$ and $x_s^2 \mathcal{O}(x_u)$ from the differential equation for $x_{ss}$ are removed. Also, if $\alpha - \beta < 1$, then there is a smooth plane bundle along $W^u(\mathbf{0})$, extending $T_{\mathbf{0}} W^{ss}(\mathbf{0}) \oplus T_{\mathbf{0}} W^u(\mathbf{0}) = \{x_s = 0\}$ over the origin; compare, for example, [HKN97]. A smooth coordinate change makes this

plane bundle constant. Terms $x_{ss}\mathcal{O}(x_u)$ are absent from the differential equation for $x_s$ after such a coordinate change. None of the coordinate changes destroys the results of the earlier coordinate changes, so that the lemma is proved. □

## B1. Exponential Expansions for the Inclination Flip

Recall that $\Sigma^{\text{in}} = \{x_s = 1\}$ and $\Sigma^{\text{out}} = \{x_u = 1\}$. The following proposition provides asymptotic expansions of the local transition map $\Phi_{\text{loc}}: \Sigma^{\text{in}} \to \Sigma^{\text{out}}$. Its proof relies on an improvement of estimates derived in [OS87, Den89, Den89b].

***Proposition B2.*** *Suppose $2\beta \neq \alpha$. Then, after a smooth local coordinate change, $\Phi_{\text{loc}}: \Sigma^{\text{in}} \to \Sigma^{\text{out}}$ has the following expression for its components $\Phi_{\text{loc}} = (\Phi^{ss}_{loc}, \Phi^{s}_{loc})$:*

$$\Phi^{ss}_{loc}(x_{ss}, x_u) = x_u^{\min\{\alpha, 2\beta\}}(\psi^{ss}(x_{ss}) + R^{ss}(x_{ss}, x_u))$$
$$\Phi^{s}_{loc}(x_{ss}, x_u) = x_u^{\beta}(1 + R^{s}(x_{ss}, x_u))$$

*The functions $\psi^{ss}, \psi^{s}$ are smooth, $\psi^{s} \neq 0$ and $\psi^{ss}(0) = 0$, if $\sigma < 2\beta$.*

*Furthermore, $R^{ss}$ and $R^{s}$ are smooth for $x_u > 0$; for some $\sigma > 0$, there exist constants $C_{k+l} > 0$ so that with $i = ss, s$*

$$\left| \frac{\partial^{k+l}}{\partial x_u^k \, \partial(x_{ss}, \mu)^l} R^i(x_{ss}, x_u) \right| \leqslant C_{k+l} x_u^{\sigma - k}$$

**Proof.** We give the proof under the assumption that $\alpha > 2\beta$. The proof for the case $\alpha < 2\beta$ is similar; compare [HKN97].

Use coordinates and notation as provided by Lemma B1 and (11). For $\tau > 0$ and $\xi_{ss}$ with $|\xi_{ss}| < 1$, let

$$x(t, \tau, \xi_{ss}) = (x_{ss}, x_s, x_u)(t, \tau, \xi_{ss})$$

be an orbit of $X_\mu$ with

$$x_{ss}(0, \tau, \xi_{ss}) = \xi_{ss}$$
$$x_s(0, \tau, \xi_{ss}) = 1$$
$$x_u(\tau, \tau, \xi_{ss}) = 1$$

These conditions uniquely define the orbit $x(t, \tau, \xi_{ss})$; see [Shi67, Den89]. We will first show the following lemma, providing estimates on $x_{ss}(t, \tau, \xi_{ss})$ and $x_s(t, \tau, \xi_{ss})$.

***Lemma B3.*** *For $k \geqslant 0$, there are positive constants $C_k$ so that, for $0 \leqslant t \leqslant \tau$ and $\mu$ near 0,*

$$\left| \frac{\partial^k}{\partial(t, \xi_{ss}, \mu)^k} x_{ss}(t, \tau, \xi_{ss}) \right| \leqslant C_k e^{-2\beta t}$$

$$\left| \frac{\partial^k}{\partial(t, \xi_{ss}, \mu)^k} x_s(t, \tau, \xi_{ss}) \right| \leqslant C_k e^{-\beta t}$$

*Furthermore, for the derivatives with respect to $\tau$,*

$$\left| \frac{\partial^k}{\partial(t, \tau, \xi_{ss}, \mu)^k} \frac{\partial}{\partial \tau} x_{ss}(t, \tau, \xi_{ss}) \right| \leqslant C_k e^{-2\beta t + (t-\tau)}$$

$$\left| \frac{\partial^k}{\partial(t, \tau, \xi_{ss}, \mu)^k} \frac{\partial}{\partial \tau} x_s(t, \tau, \xi_{ss}) \right| \leqslant C_k e^{-\beta t + (t-\tau)}$$

**Proof of Lemma B3.** To simplify the notation we write, for example, $x(t)$ for $x(t, \tau, \xi_{ss})$. Let $\delta$ be the distance of the sections $\Sigma^{\text{in}}$ and $\Sigma^{\text{out}}$ to the origin, before rescaling. Because of the applied rescaling $(x_{ss}, x_s, x_u) \mapsto (x_{ss}, x_s, x_u)/\delta$, we have

$$F^{ss}(x_{ss}, x_s, x_u)|, |F^s(x_{ss}, x_s, x_u)| \leqslant C\delta \tag{13}$$

for some $C > 0$ uniformly in $(x_{ss}, x_s, x_u, \mu)$. By the variation of constants formula

$$x_{ss}(t) = e^{-\alpha t} \xi_{ss} + \int_0^t e^{-\alpha(t-s)} F^{ss}(x(s))\, ds \tag{14}$$

$$x_s(t) = e^{-\beta t} + \int_0^t e^{-\beta(t-s)} F^s(x(s))\, ds \tag{15}$$

For $\kappa, \lambda > 0$ and a finite-dimensional vector space $E$ with norm $\|\cdot\|$, let

$$\Sigma_{\kappa, \lambda}([0, \tau], E) = \{ y \in C^0([0, \tau], E);\ \sup_{0 \leqslant t \leqslant \tau} \|y(t)\|\, e^{\kappa t + \lambda(\tau - t)} < \infty \}$$

Equipped with the norm

$$\|y\|_{\kappa, \lambda} = \sup_{0 \leqslant t \leqslant \tau} \|y(t)\|\, e^{\kappa t + \lambda(\tau - t)}$$

$\Sigma_{\kappa, \lambda}([0, \tau], E)$ is a Banach space.

Let $\mathcal{Y} = (\mathcal{Y}^{ss}, \mathcal{Y}^{s})$ be the map on $C^0([0, \tau], \mathbf{R}^2)$ that maps $(x_{ss}, x_s)$ to the right-hand side of (14), (15). Let $\mathbf{B}_R$ denote the ball of radius $R$ in $\Sigma_{\alpha,0}([0, \tau], \mathbf{R}) \times \Sigma_{\beta,0}([0, \tau], \mathbf{R})$. We claim that for $\|\xi_s\| \leqslant 1$ there exists $R > 0$ so that

- $\mathcal{Y}$ maps $\mathbf{B}_R$ inside itself,
- $\mathcal{Y}$ is a contraction on $\mathbf{B}_R$.

The fixed point of $\mathcal{Y}$, providing the orbit $x$, therefore satisfies the estimates in the statement of the lemma.

The claim is obtained by using (13) and Lemma B1. Since the arguments closely follow those in [Den89], we do not reproduce the estimates here. One treats (higher order) derivatives by differentiating (14), (15) and using the obtained identities to define a map on an appropriate weighted Banach space. Performing estimates as above, one shows that this map leaves a ball in the Banach space invariant. Therefore, derivatives satisfy the bounds given by the norm. For details we refer to [Den89]. □

To obtain more precise asymptotics, we study the functions

$$z_{ss}(u, \tau, \xi_{ss}) = e^{2\beta(\tau - u)} x_{ss}(\tau - u, \tau, \xi_{ss})$$

$$z_s(u, \tau, \xi_{ss}) = e^{\beta(\tau - u)} x_s(\tau - u, \tau, \xi_{ss})$$

for which we have the following.

***Lemma B4.*** *The limit functions*

$$z_{ss}^{\infty}(u, \xi_{ss}) = \lim_{\tau \to \infty} z_{ss}(u, \tau, \xi_{ss})$$

$$z_s^{\infty}(u, \xi_{ss}) = \lim_{\tau \to \infty} z_s(u, \tau, \xi_{ss})$$

*exist as smooth functions of* $(u, \xi_{ss})$. *For any* $0 < \sigma^{ss} < \alpha(0) - 2\beta(0)$ *and* $0 < \sigma^{s} < \min\{\alpha(0) - \beta(0), \beta(0)\}$, *there are* $C_k$ *so that for* $0 \leqslant u \leqslant \tau$ *and* $\mu$ *small*

$$\left| \frac{\partial^k}{\partial(u, \tau, \xi_{ss}, \mu)^k} (z_{ss}(u, \tau, \xi_{ss}) - z_{ss}^{\infty}(u, \xi_{ss})) \right| \leqslant C_k e^{\sigma^{ss}(u - \tau)}$$

$$\left| \frac{\partial^k}{\partial(u, \tau, \xi_{ss}, \mu)^k} (z_s(u, \tau, \xi_{ss}) - z_s^{\infty}(u, \xi_{ss})) \right| \leqslant C_k e^{\sigma^{s}(u - \tau)}$$

**Proof of Lemma B4.** We first show that

$$\left|\frac{\partial}{\partial\tau} z_{ss}(u, \tau, \xi_{ss})\right| \leqslant Ce^{\sigma^{ss}(u-\tau)} \tag{16}$$

$$\left|\frac{\partial}{\partial\tau} z_{s}(u, \tau, \xi_{ss})\right| \leqslant Ce^{\sigma^{s}(u-\tau)} \tag{17}$$

for some $C$. From this it follows that $z_{ss}^{\infty}(u, \xi_{ss}) = \lim_{\tau\to\infty} z_{ss}(u, \tau, \xi_{ss})$ and $z_{s}^{\infty}(u, \xi_{ss}) = \lim_{\tau\to\infty} z_{s}(u, \tau, \xi_{ss})$ exist and that

$$|z_{ss}(u, \tau, \xi_{ss}) - z_{ss}^{\infty}(u, \xi_{ss})| \leqslant Ce^{-\sigma^{ss}(\tau-u)}$$
$$|z_{s}(u, \tau, \xi_{ss}) - z_{s}^{\infty}(u, \xi_{ss})| \leqslant Ce^{-\sigma^{s}(\tau-u)}$$

As in the proof of Lemma B3, we simplify the notation and write, for example, $z_{ss}(t)$ for $z_{ss}(t, \tau, \xi_{ss})$. We have

$$z_{ss}(u) = e^{(2\beta-\alpha)(\tau-u)}\xi_{ss} + \int_{0}^{\tau-u} e^{(2\beta-\alpha)(\tau-u)}e^{\alpha s}F^{ss}(x(s))\, ds \tag{18}$$

$$z_{s}(u) = 1 + \int_{0}^{\tau-u} e^{\beta s}F^{s}(x(s))\, ds \tag{19}$$

One computes that

$$\begin{aligned}\frac{\partial}{\partial\tau} z_{ss}(u) &= (2\beta-\alpha)\, e^{(2\beta-\alpha)(\tau-u)}\xi_{ss} + e^{2\beta(\tau-u)}F_{ss}(x(\tau-u)) \\ &\quad + \int_{0}^{\tau-u} (2\beta-\alpha)\, e^{(2\beta-\alpha)(\tau-u)}e^{\alpha s}F_{ss}(x(s))\, ds \\ &\quad + \int_{0}^{\tau-u} e^{(2\beta-\alpha)(\tau-u)}\, e^{\alpha s}\frac{\partial}{\partial\tau} F_{ss}(x(s))\, ds \end{aligned} \tag{20}$$

$$\frac{\partial}{\partial\tau} z_{s}(u) = e^{\beta(\tau-u)}F^{s}(x(\tau-u)) + \int_{0}^{\tau-u} e^{\beta s}\frac{\partial}{\partial\tau} F^{s}(x(s))\, ds. \tag{21}$$

Lemma B1 (with (11)) and Lemma B3 yield

$$|F^{ss}(x(s))| \leqslant C_0 e^{-3\beta s}, \qquad \left|\frac{\partial}{\partial\tau} F^{ss}(x(s))\right| \leqslant C_0 e^{-3\beta s + (s-\tau)}$$

$$|F^{s}(x(s))| \leqslant C_0 e^{-2\beta s}, \qquad \left|\frac{\partial}{\partial\tau} F^{s}(x(s))\right| \leqslant C_0 e^{-2\beta s + (s-\tau)}$$

Direct estimates now prove (16) and (17); compare [Den89b]. Estimates for derivatives are obtained similarly, by differentiating (18) and (19). □

The above lemmas yield expansions,

$$x_{ss}(\tau, \tau, \xi_{ss}) = e^{-2\beta\tau}(\psi^{ss}(\xi_{ss}) + T^{ss}(\xi_{ss}, \tau)) \tag{22}$$

$$x_s(\tau, \tau, \xi_{ss}) = e^{-\beta\tau}(1 + T^{s}(\xi_{ss}, \tau)) \tag{23}$$

Here $T^{ss}$ and $T^s$ as well as their derivatives are of order $\mathcal{O}(e^{-\sigma^{ss}\tau})$ and $\mathcal{O}(e^{-\sigma^{s}\tau})$, respectively, as $\tau \to \infty$. From $x_u(0, \tau, \xi_{ss}) = e^{-\tau} = 1$ we get $\tau = -\ln x_u$. Putting this in the expansion formulas (22), (23) for $x_{ss}(\tau, \tau, \xi_{ss})$ and $x_s(\tau, \tau, \xi_{ss})$ gives the result of Proposition B2. □

## B2. Exponential Expansions for the Orbit Flip

Recall that $\Sigma^{\text{in}} = \{x_{ss} = 1\}$ and $\Sigma^{\text{out}} = \{x_u = 1\}$. Asymptotic expansions for the local transition map $\Phi_{\text{loc}}: \Sigma^{\text{in}} \to \Sigma^{\text{out}}$ are derived using analogous techniques as in the previous section. In [HKN97] such expansions are given for the case $1 < \beta < \frac{1}{2}$.

***Proposition B5.*** *Suppose $\alpha - \beta < 1$. After a smooth local coordinate change $\Phi_{\text{loc}}: \Sigma^{\text{in}} \to \Sigma^{\text{out}}$ has the following expression for its components $\Phi_{\text{loc}} = (\Phi^{ss}_{\text{loc}}, \Phi^{s}_{\text{loc}})$:*

$$\Phi^{ss}_{\text{loc}}(x_s, x_u) = x_u^{\alpha}(\phi^{ss}_{\text{loc}}(x_s) + R^{ss}(x_s, x_u)) + x_s x_u^{\beta} U^{ss}(x_s, x_u)$$

$$\Phi^{s}_{\text{loc}}(x_s, x_u) = x_s x_u^{\beta}(\phi^{s}(x_s) + U^{s}(x_s, x_u)) + x_u^{\alpha} R^{s}(x_s, x_u)$$

*The functions $\phi^{ss}$, $\phi^s$ are smooth, $\psi^{ss}$, $\phi^s \neq 0$.*

*Furthermore, $R^{ss}$, $R^s$, $U^{ss}$, $U^s$ are smooth for $x_u > 0$; for some $\sigma > 0$, there exist constants $C_{k+l} > 0$ so that, with $i = ss, s$*

$$\left| \frac{\partial^{k+l}}{\partial x_u^k \, \partial(x_s, \mu)^l} R^i(x_s, x_u) \right| \leqslant C_{k+l} x_u^{\sigma - k}$$

$$\left| \frac{\partial^{k+l}}{\partial x_u^k \, \partial(x_s, \mu)^l} U^i(x_s, x_u) \right| \leqslant C_{k+l} x_u^{\sigma - k}$$

**Proof.** The proof follows the proof of Proposition B2. We indicate the necessary steps, leaving details to the reader. Take coordinates as in Lemma B1 and (12). Consider the orbit $(x_{ss}, x_s, x_u)(t, \tau)$ with $x_{ss}(0, \tau) = 1$,

$x_s(0, \tau) = \xi_s$ and $x_u(\tau, \tau) = 1$. Using estimates as in Lemmas B3 and B4, one first shows that, for some $\omega > 0$,

$$x_{ss}(t, \tau) = \mathcal{O}(e^{-(\beta+\omega)t})$$
$$x_s(t, \tau) = e^{-\beta t}\phi(\xi_s) + \mathcal{O}(e^{-(\beta+\omega)t})$$

Similar estimates hold for derivatives. Filling in the transition time $\tau = -\ln x_u$ gives

$$\Phi^{ss}_{\text{loc}}(x_s, x_u) = \mathcal{O}(x_u^{\beta+\omega}) \tag{24}$$
$$\Phi^{s}_{\text{loc}}(x_s, x_u) = x_u^{\beta}\phi(x_s) + \mathcal{O}(x_u^{\beta+\omega}) \tag{25}$$

Sharper estimates can be obtained if $\xi_s = 0$. If $\xi_s = 0$ then the variation of constants formula yields

$$x_{ss}(t, \tau) = e^{-\alpha t} + \int_0^t e^{-\alpha(t-s)}F^{ss}(x(s))\, ds$$

$$x_s(t, \tau) = \int_0^t e^{-\beta(t-s)}F^{s}(x(s))\, ds$$

where we have written $x(s) = (x_{ss}, x_s, x_u)(s, \tau)$. We claim that for some $\omega > 0$,

$$x_{ss}(t, \tau) = ce^{-\alpha t} + \mathcal{O}(e^{-(\alpha+\omega)t}) \tag{26}$$
$$x_s(t, \tau) = \mathcal{O}(e^{-(\alpha+\omega)t}) \tag{27}$$

for some smooth function $c$ of $\mu$ with $c \neq 0$. Copying the proof of Lemma B3 one first shows that

$$x_{ss}(t, \tau) = \mathcal{O}(e^{-\alpha t}) \tag{28}$$
$$x_s(t, \tau) = \mathcal{O}(e^{-(\alpha+\omega)t}) \tag{29}$$

and

$$\frac{\partial}{\partial \tau} x_{ss}(t, \tau) = \mathcal{O}(e^{-\alpha t + (t-\tau)}) \tag{30}$$

$$\frac{\partial}{\partial \tau} x_s(t, \tau) = \mathcal{O}(e^{-(\alpha+\omega)t + (t-\tau)}) \tag{31}$$

with similar estimates for higher-order derivatives. Here one uses Lemma B1 and (12). In order to obtain the expansion (that is, to determine the leading term) for $x_{ss}$, define

$$z_{ss}(u, \tau) = e^{\alpha(\tau - u)} x_{ss}(\tau - u, \tau)$$

One can show that

$$z_{ss}(u, \tau) = z_{ss}^{\infty}(u) + \mathcal{O}(e^{\sigma(u-\tau)}) \tag{32}$$

for a smooth function $z_{ss}^{\infty}$ and some $\sigma > 0$ (with similar estimates for derivatives). Indeed, following the reasoning in the proof of Lemma B4, one computes

$$\frac{\partial}{\partial \tau} z_{ss}(u, \tau) = \int_0^{\tau - u} e^{\alpha s} \frac{\partial}{\partial \tau} F^{ss}(x(s))\, ds + e^{\alpha(\tau - u)} F^{ss}(x(\tau - u))$$

Using estimates

$$|F^{ss}(x(s))| \leqslant Ce^{-2\alpha s}$$

$$\left| \frac{\partial}{\partial \tau} F^{ss}(x(s)) \right| \leqslant Ce^{-2\alpha s + (s - \tau)}$$

which follow from (28), (29), (30), (31) and Lemma B1, one sees that

$$\left| \frac{\partial}{\partial \tau} z_{ss}(u, \tau) \right| \leqslant Ce^{\sigma(u-\tau)}$$

for some $C > 0$, $\sigma > 0$. The remainder of the proof of (32) and, hence, (26) goes as in the proof of Lemma B4. With $\tau = -\ln x_u$, one gets from (26)

$$\Phi_{\text{loc}}^{ss}(0, x_u) = cx_u^{\alpha} + \mathcal{O}(x_u^{\alpha + \omega}) \tag{33}$$

$$\Phi_{\text{loc}}^{s}(0, x_u) = \mathcal{O}(x_u^{\alpha + \omega}) \tag{34}$$

Here $c$ is a smooth nonvanishing function of $\mu$.

Combining (24), (25), (33) and (34) implies the result. □

## ACKNOWLEDGMENTS

The authors thank H. Kokubu for fruitful discussions and B. Oldeman for several very helpful comments on the bifurcation diagrams of an early version of this paper. We are grateful for hospitality and support from the Institute for Mathematics and Its Applications in Minneapolis, the University

of Bristol, Freie Universität Berlin, and the Schwerpunktprogramm "Ergodentheorie, Analysis and effiziente Simulation dynamischer Systeme" of Deutsche Forschungsgemeinschaft.

## REFERENCES

[CDF90] Chow, S.-N., Deng, B., and Fiedler, B. (1990). Homoclinic bifurcation at resonant eigenvalues, *J. Dyn. Diff. Eq.* **2**, 177–244.

[Den89] Deng, B. (1989). The Shil'nikov problem, exponential expansion, strong $\lambda$-lemma, $C^1$-linearization, and homoclinic bifurcation. *J. Diff. Eq.* **79**, 189–231.

[Den89b] Deng, B. (1989). Exponential expansion with Šil'nikov's saddle-focus. *J. Diff. Eq.* **82**, 156–173.

[Den90] Deng, B. (1993). Homoclinic twisting bifurcations and cusp horseshoe maps. *J. Dyn. Diff. Eq.* **5**, 417–467.

[DCFKSW97] Doedel, E. J., Champneys, A. R., Fairgrieve, T. F., Kuznetsov, Yu. A., Sandstede, B., and Wang, X. (1997). AUTO 97: Continuation and bifurcation software for ordinary differential equations (with Hom-Cont). http://indy.cs.concordia.ca/auto/

[DRS91] Dumortier, F., Roussarie, R., and Sotomayor, J. (1991). *Bifurcations of Planar Vector Fields, Nilpotent Singularities and Abelian Integrals*, Lecture Notes in Mathematics **1480**, Springer-Verlag, Berlin.

[GAKS93] Gaspard, P., Arnéodo, A., Kapral, R., and Sparrow, C. (1993). Homoclinic chaos, *Physica D* **62** (Special Issue).

[Hom96] Homburg, A. J. (1996). *Global Aspects of Homoclinic Bifurcations of Vector Fields*, Memoirs of the AMS **578**.

[HKK94] Homburg, A. J., Kokubu H., and Krupa, M. (1994). The cusp horseshoe and its bifurcations in the unfolding of an inclination flip homoclinic orbit. *Ergod. Th. Dynam. Syst.* **14**, 667–693.

[HKN97] Homburg, A. J., Kokubu, H., and Naudot, V. (1997). Homoclinic-doubling cascades (preprint).

[HY99] Homburg, A. J. and Young, T. (1999). Universal scalings in homoclinic doubling cascades (preprint).

[KKO93a] Kisaka, M., Kokubu, H., and Oka, H. (1993). Bifurcations to $N$-homoclinic orbits and $N$-periodic orbits in vector fields. *J. Dyn. Diff. Eq.* **5**, 305–357.

[KKO93b] Kisaka, M., Kokubu, H., and Oka, H. (1993). Supplement to homoclinic-doubling bifurcation in vector fields. In Bamon, R., Labarca, R., Lewowicz, J., and Palis, J., eds., *Dynamical Systems*, Longman, pp. 92–116.

[KKO95] Kokubu, H., Komuro, M., and Oka, H. (1995). Numerical study of a piecewise affine vector field (private communication).

[KKO96] Kokubu, H., Komuro, M., and Oka, H. (1996). Multiple homoclinic bifurcations from orbit flip. I. Successive homoclinic-doubling. *Int. J. Bif. Chaos* **6**, 833–850.

[KN97] Kokubu, H., and Naudot, V. (1997). Existence of infinitely many homoclinic-doubling bifurcations from some codimension-three homoclinic orbits. *J. Dyn. Diff. Eq.* **9**, 445–462.

[Ko95] Koper, M. (1995). Bifurcations of mixed-mode oscillations in a three-variable autonomous Van der Pol–Duffing model with a cross shaped phase diagram. *Physica D* **80**, 72–94.

[KR96] Krauskopf, B., and Rousseau, C. (1997). Codimension-three unfoldings of reflectionally symmetric vector fields. *Nonlinearity* **10**, 1115–1150.

[Mon96] Montealegre, M. (1996). *Bifurcações homoclínicas para selas em* $\mathbf{R}^3$ *com ressonância nas direções principas* (*Homoclinit Bifurcations of Saddles in* $\mathbf{R}^3$ *with Resonance along Principal Directions*), Ph.D. thesis, Universidada de São Paulo; personal communication with J. Sotomayor (1998).

[Nii96] Nii, S. (1996). *N*-homoclinic bifurcations for homoclinic orbits changing their twisting. *J. Dyn. Diff. Eq.* **8**, 549–572.

[Nau96a] Naudot, V. (1996). *Bifurcations Homoclines des Champs de Vecteurs en Dimension Trois*, Ph.D. thesis, l'Université de Bourgogne, Dijon.

[Nau96b] Naudot, V. (1996). Strange attractor in the unfolding of an inclination flip homoclinic orbit. *Ergod. Th. Dynam. Syst.* **16**, 1071–1086.

[Nau98] Naudot, V. (1998). A strange attractor in the unfolding of an orbit flip homoclinic orbit (preprint).

[OKC00] Oldeman, B. E., Krauskopf, B., and Champneys A. R. (2000). Death of period-doublings: Locating the homoclinic-doubling cascade. *Physica D* **146**, 100–120.

[OKC00b] Oldeman, B. E., Krauskopf, B., and Champneys A. R. (2000). Numerical unfolding of codimension-three resonant homoclinic flip bifurcations, Applied Nonlinear Mathematics Research Report 2000.7, University of Bristol, submitted for publication.

[OS87] Ovsyannikov, I. M., and Shil'nikov, L. P. (1987). On systems with saddle-focus homoclinic curve. *Math. USSR Sbornik* **58**, 557–574.

[Rob89] Robinson, C. (1989). Homoclinic bifurcation to a transitive attractor of Lorenz type. *Nonlinearity* **2**, 495–518.

[Rob92] Robinson, C. (1992). Homoclinic bifurcation to a transitive attractor of Lorenz type. II. *SIAM J. Math. Anal.* **23**, 1255–1268.

[RR96] Roussarie, R., and Rousseau, C. (1996). Almost planar homoclinic loops in $\mathbf{R}^3$. *J. Diff. Eq.* **126**, 1–47.

[Ryc90] Rychlik, M. R. (1990). Lorenz attractors through Sil'nikov-type bifurcation. Part I. *Ergod. Th. Dynam. Syst.* **10**, 793–821.

[San93] Sandstede, B. (1993). *Verzweigungstheorie Homokliner Verdopplungen*, Ph.D. thesis, Freie Universität Berlin, Institut für Angewandte Analysis und Stochastic, Report No. 7, Berlin.

[San97] Sandstede, B. (1997). Constructing dynamical systems having homoclinic bifurcation points of codimension two. *J. Dyn. Diff. Eq.* **9**, 269–288.

[Shi65] Shil'nikov, L. P. (1965). A case of the existence of a countable number of periodic motions. *Soviet Math. Dokl.* **6**, 163–166.

[Shi67] Shil'nikov, L. P. (1967). On the Poincaré–Birkhoff problem. *Math. USSR Sbornik* **3**, 353–371.

[Ste58] Sternberg, S. (1958). On the structure of local homeomorphisms of Euclidean *n*-space II. *Am. J. Math.* **80**, 623–631.

[Yan87] Yanagida, E. (1987). Branching of double pulse solutions from single pulse solutions in nerve axon equations. *J. Diff. Eq.* **66**, 243–262.

[YA83] Yorke, J. A., and Alligood, K. T. (1983). Cascades of period doubling bifurcations: A prerequisite for horseshoes. *Bull. AMS* **9**, 319–322.

[ZN98] Zimmerman, M. G., and Natiello, M. A. (1998). Global homoclinic and heteroclinic bifurcations close to a twisted heteroclinic cycle. *Int. J. Bif. Chaos* **8**(2), 359–376.

*Printed in Belgium*